

## **PHAS0052: Group 11 Final Report**

Proof-of-concept of Thermally Contrasted Lateral Flow Assay Using  
Photothermal Heating From Magnetic Nanoparticles and Thermochromic  
Sheets for Limit of Detection Enhancement

Sean MacBride, Ivan Popov, Jennifer Lin, Grace Hymas, Amritpal Basi, Abigail Goh,  
Anja Rellstab, Wenhao Wu

March 19, 2019

University College London, London, WC1E 6BT, United Kingdom

# Contents

<b>Contents</b>	<b>1</b>
<b>1 Executive Summary</b>	<b>3</b>
<b>2 Distribution of Work</b>	<b>5</b>
<b>3 Introduction</b>	<b>7</b>
3.1 Lateral Flow Assays . . . . .	7
3.1.1 Thermally Contrasted Lateral Flow Assays . . . . .	8
3.1.2 Types of Lateral Flow Assays . . . . .	9
3.2 Membrane Selection . . . . .	10
3.3 Quantifying Results with a Mobile Phone Application . . . . .	11
3.4 Magnetic Nanoparticles . . . . .	12
3.5 Nanoparticles Photothermal Heating . . . . .	13
3.6 Gold Nanoparticles . . . . .	13
3.7 Lasers and Nanoparticles in Tandem with Diagnostic Testing . . . . .	14
3.8 Thermochromic Sheet Application . . . . .	14
<b>4 Methods and Materials</b>	<b>15</b>
4.1 Membrane Selection . . . . .	15
4.2 Membrane Preparation . . . . .	15
4.3 Experimental Setup . . . . .	17
4.4 Experimental Method: Membrane Laser Exposure . . . . .	17
<b>5 Discussion</b>	<b>20</b>
5.1 Data Analysis . . . . .	20
5.2 Limit of Detection . . . . .	25
5.2.1 Linear Trend . . . . .	26
5.2.2 Logarithmic Trend . . . . .	28
5.2.3 Square Root Trend . . . . .	30
<b>6 Conclusion</b>	<b>36</b>
6.1 Summary of Findings . . . . .	36
6.2 Improvement of Findings . . . . .	37

6.3	Evaluation of project . . . . .	37
6.4	Final Summary . . . . .	38
<b>7</b>	<b>Acknowledgements</b>	<b>39</b>
<b>Bibliography</b>		<b>40</b>
<b>8</b>	<b>Appendix</b>	<b>44</b>
<b>List of Figures</b>		<b>45</b>
<b>List of Tables</b>		<b>47</b>
8.1	Python Scripts for Data extraction and Analysis . . . . .	47
8.1.1	Fe <sub>3</sub> O <sub>4</sub> . . . . .	47
8.1.2	Zn <sub>0.4</sub> Fe <sub>2.6</sub> O <sub>4</sub> . . . . .	55
8.2	Finances . . . . .	61
8.2.1	Total Covered Costs . . . . .	61
8.2.2	Membranes . . . . .	61
8.2.3	Thermochromic Sheets . . . . .	62
8.3	Risk Assessment . . . . .	63
8.4	Lab Book . . . . .	66
8.5	Minutes . . . . .	83
8.5.1	15/1 Meeting . . . . .	83
8.5.2	25/1 Meeting . . . . .	84
8.5.3	1/2 Meeting . . . . .	85
8.5.4	6/2 Meeting . . . . .	86
8.5.5	8/2 Meeting . . . . .	86
8.5.6	8/3 Meeting . . . . .	88
8.5.7	14/3 Meeting . . . . .	89

# Chapter 1

## Executive Summary

*by Sean MacBride, Amritpal Basi, Jennifer Lin*

The aim of this project was to detect the lower limit of detection in nitrocellulose membranes when concentrated with various metallic nanoparticles. Information on membranes, nanoparticles, thermochromic sheets, and applications for the research was gathered in the form of a literature review. Alongside background research, information about laboratory use and limitations were discussed with Prof. Nguyen and time slots were allocated with the appropriate risk assessments signed. This proved to be one of the most difficult tasks of the project, as UCL safety guidelines inhibited the use of the optimal laser. An appropriate laser on the second-floor lab within the UCL physics building with an excitation wavelength of 780nm and a power output of 40mW was used. The nitrocellulose membranes utilized were yellow and blue membranes from Bio-Rad with a pore size of  $0.45\mu\text{m}$  and  $0.2\mu\text{m}$  respectively.

Membranes with various concentrations of nanoparticle solution were synthesized. Initial tests were done using a laser, membrane and thermochromic sheet setup without a thermal camera for empirical confirmation of the qualitative results which were observed as changes to the thermochromic sheet. Upon the conclusion of these tests, it was determined that the current setup would yield minimal qualitative results without the use of a thermal camera. The next round of tests was fifteen-minute exposures of the membranes at different concentrations. After analysis of the thermal camera readings, it was seen that a plateau state was reached after three minutes of heating, and therefore a three-minute exposure was sufficient to reach the maximum temperature of the membrane with a solution. The third and final round of tests was with the three-minute exposure of membranes of various colors and solutions to the laser. This round of testing yielded the bulk of our results.

The data extracted from the tests was in the form of thermal images. The temperature of the hotspot was extracted using Testo IRSoft software. These temperatures were then analyzed and plotted using Python and Matplotlib [1].

Unfortunately, due to difficulty in initial hardware acquisition and limited test runs, data was inconclusive for both the detection of a lower limit of detection. and a difference in heating between different membranes. Further test runs using these techniques would allow refinement of results with thermochromic sheets. The method used here could similarly be applied to lateral

flow assays (LFA's), to allow for the testing of certain diseases and cultures in the body. Furthermore, these results could be integrated into a mobile application where an easily accessible phone could be utilized to provide semi-qualitative and quantitative results for LFA's, advising the user of appropriate action.

## Chapter 2

# Distribution of Work

Member	Work performed over course of project	Authorship pieces in report
Sean MacBride	Lab work and coordination, data analysis, and image testing	Executive summary, introduction, distribution of work, methods and materials, discussion, report formatting and editing
Grace Hymas	Lab work, data analysis, and poster work	Methods, discussion, report editing, and data analysis
Ivan Popov	Communication Chair, data analysis, 3D imaging, Lab work, Python code	Introduction, Discussion
Amritpal Basi	Application design and research , Literature Review, Nitrocellulose membrane research for purchase, software research	Introduction, Conclusion
Jennifer Lin	Literature review, diseases and infections presentation research, poster work	Executive Summary, Introduction, conclusion, report editing and formatting
Abigail Goh	Literature review, diseases and infections presentation research, email correspondence	Introduction, methods and materials
Anja Rellstab	Literature review, poster work, diseases and infections presentation research, app design	Introduction, conclusion
Wenhao Wu	Literature review, diseases and infections presentation research, email correspondence	Abstract, introduction, methods

Table 2.1: Table detailing the work done by individual group members on practical and logistical, laboratory, and report based work

# Chapter 3

## Introduction

by Abby Goh, Anja Rellstab, Wenhao Wu, Amritpal Basi, Sean MacBride, and Jennifer Lin

### 3.1 Lateral Flow Assays

Point-of-care testing (POCT) allows for a prompt medical diagnosis at the time and place of a patient's care and as a result POCT has become one of the most popular methods of clinical analysis. LFAs are POCT based devices consisting of a sample pad, nitrocellulose membrane and test/control lines that can be used for detecting the presence or absence of pathogens, biomarkers or contaminants in a solution [2].

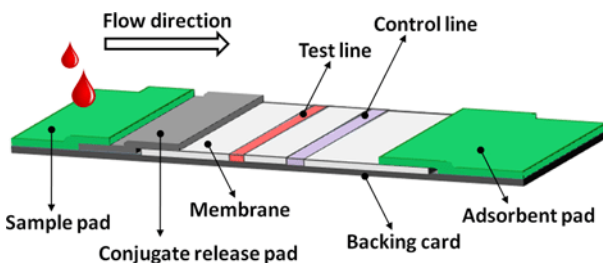


Figure 3.1: Illustration of a typical configuration of a Lateral Flow Assay composed of a sample pad, membrane, conjugate release pad, backing card, absorbent pad, test line and control line by Dr. Katarzyna M. Koczuła [2]

One of the most common forms of LFAs are pregnancy tests which test for the presence of anti- $\beta$  hCG antibodies in urine. However LFAs have actually been employed in numerous different industries, as quality control tests and even used as a cheap alternative for early disease detection of several fatal diseases such as Dengue and Zika [3]. There have also been recent efforts to produce LFAs for multiplex detection LFAs, testing for 2 target analytes with one test, which could lead to testing of several diseases at a time.

LFAs are an ideal tool for detection due to their low development cost, prompt results, long shelf life and ease of use by patients without the help of a healthcare professional. Versatility is another component of LFAs as tests can be performed on various biological samples such as

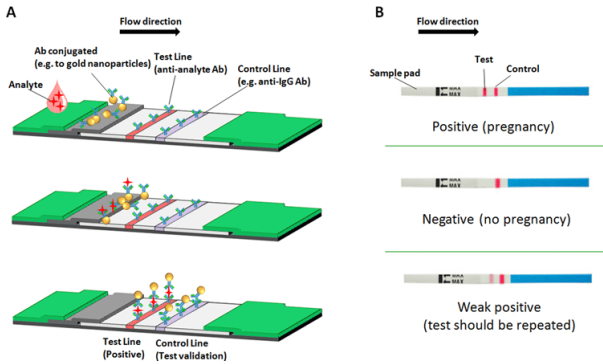


Figure 3.2: Illustration of the operation of a Lateral FLow Assay by (Dr.) Katarzyna M. Koczuła [2]

plasma, sweat, saliva, blood and more with only requiring a small sample for each test. These promising attributes mean LFA's are projected to increase in use at a Compound annual growth rate of 8.2% by 2022 [4].

Although LFAs have many advantages, there are several shortcomings such as inconsistent reproducibility, low biomolecule affinity, pre-treatment of the samples may be time consuming and the analysis time is dependent on the nature of the sample. One major disadvantage is its sensitivity and a number of possible solutions have been tested to address this such as the use of immunomagnetic particles and beads [5] [6], silver enhancement [7], magnetic nanoparticles and even SERS [3]. Many researchers are developing ways to increase sensitivity with microfluidics, biobar codes and enzyme based immunoassay technologies [8].

The aim of this project is to explore a new way of detection using nitrocellulose membranes in order to increase the sensitivity through the use of metallic nanoparticles, excited by a laser, to quantify and increase the limit of detection of the target analyte. The limit of detection refers to the minimum concentration of the magnetic nanoparticles in which the result is distinguishable from the control results, i.e. a test strip absent of nanoparticles. This ultimately would lead on to a detection method that works as a lateral flow assay with greater sensitivity and where the change of colour in the thermochromic sheet reflects the concentration of analyte in the sample.

### 3.1.1 Thermally Contrasted Lateral Flow Assays

This experiment will be focusing on the Proof-of-Concept of thermally contrasted LFAs to improve sensitivity of LFAs. As this is the preliminary stages, no target antibody has been introduced yet and the solution used is purely magnetic nanoparticles of varying concentrations applied onto a nitrocellulose membrane. These coated membranes are then exposed to a laser, causing thermal activation in the magnetic particles and hence, an increase in temperature. In this experiment, a higher concentration of nanoparticles implies a higher concentration of antigen, hence it is expected that the temperature of the test strip increases with the concentration.

By inserting thermochromic sheets under the test strip membranes, the concentration of MNPs in the solution can be quantified. These thermochromic sheets shift colour due to the change in temperature and from the extent of temperature change they serve as a representation

of the concentration of the particles (and therefore also the analytes) visually. The colour change could be read both qualitatively and quantitatively by employing an optical strip reader or a software with a suitable colour calibration curve that is compatible on a mobile phone.

### 3.1.2 Types of Lateral Flow Assays

There are two main types of LFAs, sandwich assays and competitive assays. Sandwich Assays are used to measure the amount of analyte between two layers of antibodies and are generally used for analytes with larger molecular weights. This is done by applying a known analyte onto the sample pad. The sample then migrates across the membrane and will bind with the line of immobilised antibodies, or the test line if the target antigen is present, causing a visible change, such as the appearance of a coloured line. If not, no visible test line will appear as the sample continues to migrate across the membrane. LFAs usually have a control line as well as a test line, to ensure that the sample has travelled completely across the membrane. As the sample travels across the control line, there should be a colour change regardless of whether the target analyte is present or not [2].

Competitive Assays are used to detect analytes of smaller molecular weights and work under the concept that unlabelled and labelled analytes compete with each other to bind with the antibodies. If the target analyte is present, the concentration of the antigen in the sample increases and the antigens block some of the antibodies, preventing the labelled analytes from binding with them. As a result, the visible coloured test line will fade [9]. The types of Lateral Flow Assays can be seen in figure 3.3 [10].

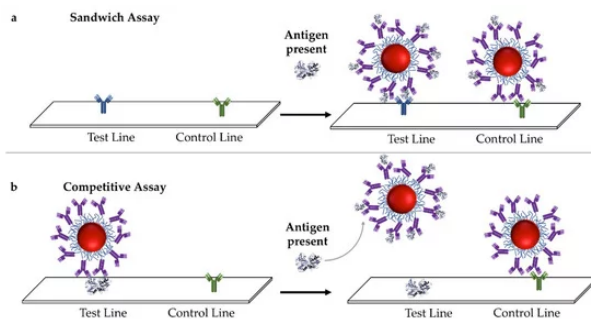


Figure 3.3: An illustration of a Sandwich assay and a Competitive assay with the following reaction in the presence of an antigen [10].

LFAs for multiplexed detection are also being developed which could detect multiple target analytes simultaneously within one single test [11]. These Multiplex Assays work under the concept that colour coded magnetic beads, or microspheres, which are coated in specific antibodies and the analyte concentration can be distinguished by looking at the amount of each coloured beads at the end of the test [12]. They have yet to be tested commercially but look promising in the research scale [13]. This, along with further research could potentially remove or reduce the tendency for cross reactivity within LFA's.

### 3.2 Membrane Selection

Membranes are the focus of this experiment as they are one of the most essential parts of an LFA, in charge of allowing the sample to flow continuously through from the sample to absorbant pad and react with the antibody on the reaction area, thus shaping the initial sensitivity of the assay. Extensive research and preparation are needed before a membrane is selected and is ready for an experiment and there are several conditions taken into account when selecting the best membrane such as pore size, porosity and thickness. Pore size and porosity contribute to determining the capillary flow rate.

As observed by H Shamloo Ahmadi et al [14], in current LFA designs that are studied, tested and available, the most commonly used membranes are the nitrocellulose membranes despite their fragility and high flammability. Although Polyvinylidene difluoride (PVDF) membranes seem to possess far superior properties, such as their higher binding capacity, sensitivity and durability. PVDF and nylon are not recommended for direct applications in LFAs [14] due to their natural properties including high hydrophobicity which needs activation before reacting with antibodies, and low capillary velocity, restricting the distance travelled by analyte.

Smaller pore sizes result in a slower capillary rate, but in turn provide a higher sensitivity by allowing for more time for target analytes to bind to the antibodies. Pore sizes smaller than  $3\mu\text{m}$  however would be too slow to be effective in LFAs as discovered during membrane developments by Millipore [15]. Thickness and porosity control the amount of liquid required to fill the pore structure and ensure good signal visibility. Uniform wetting of the membranes is also essential for an accurate signal, to avoid significant discrepancies in output signal readings when measuring protein concentration in the target sample.

In a study by L.H Mujawar et al. [16], various brands of nitrocellulose membranes and their uniformity of biomolecule distribution were investigated to aid with membrane selection. Porous membranes, such as nitrocellulose, which is used in our experiment has a lower limit of detection as compared to 2D materials such as glass. By evaluating the printing and distribution of the antibody on membranes of 3 different manufacturers; GE Whatman, Sartorius-Stedim Biotech and Grace-Biolabs to analyse the uniformity of drops on each membrane. The distribution of the final signal was evaluated using the concentric ring overlay method by using high-speed cameras to investigate wettability and fluid flow and confocal laser scanning microscopy to evaluate the homogeneity of solution distribution both throughout the droplet and across the thickness of the membrane. Overall, Grace-Biolabs membranes produced the most homogeneous spots across the membrane which could be due to its hydrophobicity and fluid flow. However, due to time constraints, limited budget and a selective list of membrane suppliers, Bio-Rad membranes are used in this experiment.

With regards to membrane preparation, timing is crucial for membrane's humidity calibration. If the nitrocellulose membrane is too dry this results in non-uniform lines on the striping. If the membrane is too wet the test line is widened; consequentially the sensitivity and signal intensity are reduced as advised by Nanocomposix [17]. After equilibrating the membrane in a transfer buffer for 8-12 hours, the test and control lines can be imprinted onto the membrane,

however, this striping is not required for the experiment in this project.

### 3.3 Quantifying Results with a Mobile Phone Application

Quantifying the LFA data and results is one of the hardest aspects of this experiment. Figuring out a way to do this so that it is easy, accessible and affordable would mean that there would be more future applications and could be introduced to health care in developing countries.

One company that has already developed an application compatible with Android and IOS devices is Mobile Assay. Their application, a form of mobile diagnostic LFA test strip reader, allows users to read rapid diagnostic test results whilst also using cloud storage to collect their past data and get more detailed results online. The company currently targets their app towards smallholder farmers in Africa and their technology is specialised to test food safety by detecting toxic moulds in seeds and grains [18].

So far the contamination of Aflatoxin, Fumonisin, Filariasis, Onchocerciasis, Schistosomiasis as well as the endemic disease Malaria have been validated in this way. All of these maladies have severe adverse effects on humans and some can be fatal if left untreated.

Another smartphone lateral flow reader available is AppDx provided by Abingdon Health [19]. This application is also compatible with both Android and IOS devices and allows the user to set data criteria such as testing locations, times and dates. This criteria can also be used to help users pinpoint past data sets that have already been taken and stored by the application.

Both applications work under the same principle. The app is downloaded, a sample is provided for testing and the assay is run. The assay is then read by the phone or tablet and results are given within minutes and these can be synced between the cloud and other devices and stored.

To ensure accurate results, Mobile Assay has built in advanced light compensation and camera linearity to provide accurate results in different ambient conditions. They have also been able to pair their app with all rapid diagnostic tests, lateral flow test strips and also colour metric strips. Which proves that LFA's are very easily integrated into technology.

One very useful feature is that all tests are time stamped and geo-tagged allowing for farmers to pinpoint exact crops that have been tested on a map. Similar to AppDx, ranges can be set and notifications will alert a user to tests that come back outside of this allowed or safe range. Another great feature is the ability to export all date via DF, Excel or XML.

The backbone of being able to read the LFA's with digital technology comes from using Mobile Image Ratiometry (MIR) [20] and Quantitative Ratiometric Pixel Density Analysis (QRPDA). For MIR to produce accurate results a calibration or standard curve needs to be established so that all future results can be quantised by comparing the concentrations of analyte present in the current test with the calibration curves. To further analyse the concentrations more exactly the National Institute of Health has a processing software, Image-J [21], which allows users to subtract background, select specific signal bands, plot pixel density ratios of these bands and find the area under them to output the quantitative results [22].

### 3.4 Magnetic Nanoparticles

Nanoparticles are a diverse class of microscopic particles with units of dimensions measured in the nanometer scale. They are useful due to the fact that they bridge the gap between bulk materials and molecular structures due to their intermediate size. One main property of nanoparticles is their high surface area to volume ratio which provides high driving force in diffusion process, especially at an elevated temperature. Due to the diffusive property, the metallic nanoparticles bound with the analytes and achieve coalescence within a shorter time scale than bulk materials. This aggregation process is known as sintering where the small particles are welded together [23].

Nanoparticles are further classified by their size, shape, and material properties. The size of these particles typically ranges from 10nm – 100nm which are classified as the chemical and physical properties are often size dependent [24]. The shape of the nanoparticles are also classified since it varies the surface area to volume ratio, therefore alters the behaviour in the sintering process. The shape classifications of nanoparticles is shown in 3.4. From the solid morphology classifications, 0D indicates particles with regular three dimensional shapes including spheres, 1D indicates nanorods, 2D indicates nanodisks, and 3D indicates nanostars. The synthesis of nanoparticles could be achieved by employing nucleation theory to control the growth rate of the particles. In addition, the shape of the nanoparticles could be engineered by altering the concentration of the growth agent which synthesises the nanoparticles [25]. With the variation of different sizes and selection of materials used, nanoparticles could be specifically engineered in application to various fields including cosmetics, renewable energies, and medicine [26].

Magnetic nanoparticles (MNPs) are a subclass of nanoparticles which have high magnetic susceptibility therefore interacts with the external magnetic field as they contain magnetic materials such as iron, cobalt, nickel, and their compounds. An example of magnetic nanoparticle is iron oxide. The magnetic property of MNPs also varies by particle size. At nanoscale dimension, iron oxide nanoparticles become superparamagnetic which is a useful property for biomedical usage as these particles align with the the magnetic field. Typical applications of MNPs include cancer treatments to target cancerous cells using magnetic resonance [27].

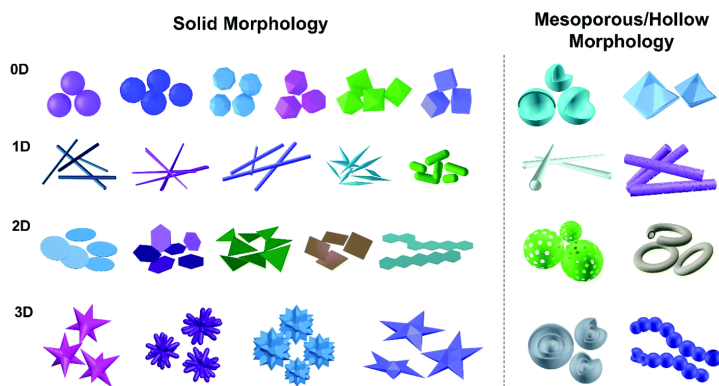


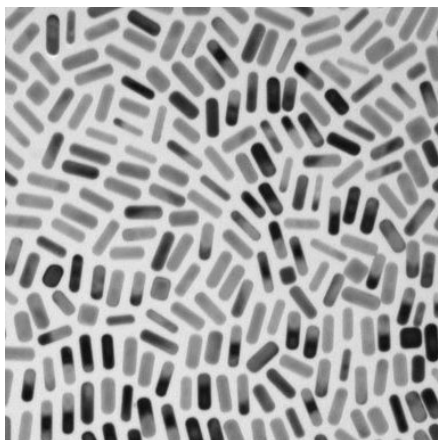
Figure 3.4: Nanoparticles shape classification [28].

### 3.5 Nanoparticles Photothermal Heating

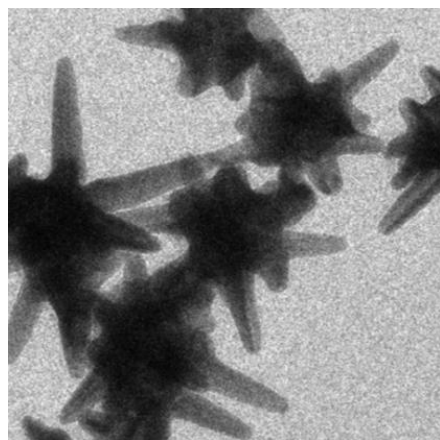
Nanoparticles made up of metallic materials are very efficient in absorbing light [29]. This means that a single nanoparticle is able to absorb a large amount of photons, therefore promoting the metal atoms in the nanoparticles to an excited state. Arising from photoelectric effect, when a certain quantised energy of photons, higher than the metal work function, is given to the nanoparticles, electrons will be released from the metallic nanoparticles. As the nanoparticles relax back to the ground state, they release heat energy through the vibrational modes. This property of metallic nanoparticles makes them very good candidates for photothermal heating in conjunction with the use of laser.

### 3.6 Gold Nanoparticles

Gold nanoparticles have metal coatings, which means that with their high electric conductivity, they are very efficient in absorbing light and could be rapidly excited due to exposure to EM radiation. In this project, gold-coated magnetic nanoparticles of two different shape classifications are used: Nanorods (Solid Morphology 1D from Figure 4) and Nanostars (Solid Morphology 3D from Figure 4). Gold nanoparticles (Fig. 3.5) are used as specimen for positive results since gold is an inert transition metal, which means that it does not easily undergo chemical reaction with the environment, therefore eliminating heating of the nanoparticles due to non-photothermal processes [30]. Gold nanorods (Fig. 3.5a) is chosen as the control sample because of its rapid photothermal heating in conjunction with laser heating [31]. Gold nanostars (Fig. 3.5b), on the other hand, is chosen due to its susceptibility to photothermal heating under a low power laser radiation [32].



(a) Gold Nanorods [33]



(b) Gold Nanostars [34]

Figure 3.5: The shapes of the gold nanoparticles used for the control samples indicating positive results.

### **3.7 Lasers and Nanoparticles in Tandem with Diagnostic Testing**

Although LFAs have many advantages, there are several shortcomings such as inconsistent reproducibility, low biomolecule affinity, pretreatment of the samples may be time consuming and the analysis time is dependent on the nature of the sample. The major downfall is the sensitivity and several of the experiments above have addressed this in a number of ways, with the use of immunomagnetic particles and beads, silver enhancement, magnetic nanoparticles and even SERS. Many researchers are developing ways to increase sensitivity with microfluidics, biobar codes and enzyme based immunoassay technologies [8]. In this experiment however, the sensitivity of LFAs hope to be improved by the use of magnetic nanoparticles, excited by a laser, to quantify and increase the detection limit of the target analyte.

To understand how magnetic nanoparticles could be employed with laser to improve detection limit, it is important to recall the mechanism of laser. Laser is a device which amplifies the original emitted electromagnetic radiation signal. The radiation emitted by a laser is monochromatic and carries momentum [35]. Optical radiation from the laser exerts radiation pressure as the momentum is transferred to an object. Monochromic signal prevents the dispersion effects caused by varied frequencies therefore ensures that the momentum transfer is consistent. The effect of the radiation pressure is amplified in small objects e.g. nanoparticles as these particles experience a larger acceleration due to the momentum transfer. Radiation pressure is a useful property of laser [36], and can be applied in such a way that allow optical tweezers to stretch and deform microscopic objects.

Of the nanoparticles mentioned above, magnetic nanoparticles interact directly with the electromagnetic radiation of the laser. As these particles are exposed to a laser, the nanoparticles oscillate such that they align with the external magnetic field [37]. These magnetic nanoparticles have a wavelength smaller than that of the radiation and so both the contribution from the oscillating magnetic field from the plane wave and the momentum transfer from the radiation to the particles results in the nanoparticles emitting thermal energy. This phenomenon is known as thermal activation where the temperature of the nanoparticle sample is increased [38]. In addition to the nanoparticles interacting with the magnetic field of laser radiation, they also exert heat due to their photothermal property (see Nanoparticles Photothermal Heating). This is important aspect in reading the LFA results as a higher concentration of nanoparticles implies a higher concentration of antigen, so the final temperature of the test strip will be higher than if the concentration was low.

### **3.8 Thermochromic Sheet Application**

The sensitivity of the LFA's could be increased by inserting thermochromic sheets under the test strip membranes. These thermochromic sheets shift colour due to the change in temperature and from the extent of temperature change they serve as a representation of the concentration of the particles (and therefore also the analytes) visually. The colour change could be read both qualitatively and quantitatively by employing an optical strip reader or a software with a suitable colour calibration curve that is compatible on a mobile phone.

# Chapter 4

## Methods and Materials

by Grace Hymas, Abby Goh, Sean MacBride, and Wenhao Wu

### 4.1 Membrane Selection

Higher powered lasers were recommended for use by Thanh Nguyen. Lasers with an energy output greater than 300mW were deemed optimal by Thithawat Trakoolwilaiwan. Lasers of this energy are prohibited for use of UCL undergraduate students, although they were readily available in the physics labs at UCL. As a result, a laser of much lower energy than desired was used in this experiment.

Based on the manufacturers recommended by Nanocomposix and the type of products available on their websites, information was initially inquired on membranes made by MDI(Advanced Microdevices) from two different, pore size based application classifications listed by MDI. These membranes had pore sizes of  $5\ \mu\text{m}$  and  $12\ \mu\text{m}$  and flowing times of 180 sec and 150 sec. The membranes were also white in colour which was optimal as no laser absorption by the membrane would occur.

However due to the time limitations,  $15 \times 9.2\ \text{cm}$  pre-cut nitrocellulose membranes of pore size  $0.45\ \mu\text{m}$  (yellow) and the  $0.2\ \mu\text{m}$  (blue) pore-size nitrocellulose membrane roll made by BIO-RAD were ordered. Since the hydrodynamical sizes of the nanoparticles used in experiment were around 100 nm, which is significantly smaller than our membrane pore size, the differences in magnitude between the initially selected membrane and the membrane that were actually ordered would not have an significant influence on the overall experimental results in terms of the point of interest in our investigation.

### 4.2 Membrane Preparation

In this experiment, Iron Oxide and Zinc Ferrite magnetic nanoparticles were used, with 2 different sizes for each type. Gold NanoRods and NanoStars were also used as control nanoparticles due to their known strong temperature change with laser exposure. The nanoparticle properties, mostly flow rate, will depend on size and so testing with different magnetic nanoparticles

determined which ones were most favourable for this experiment. For Iron Oxide magnetic nanoparticles, small particles had a size of  $10.40 \pm 2.60$  nm while the large particles had a size of  $13.2 \pm 2.10$  nm. The Zinc Ferrite particles of large and small sizes were  $15.13 \pm 2.25$  nm and  $11.00 \pm 1.80$  nm respectively.

The magnetic nanoparticles were then diluted with water to produce  $1000\mu\text{l}$  solutions of various different concentrations to find the detection limit in the following way. Using European Instruments Pipetman H3X018102 and CL50215 of volumes  $0.5\text{-}100\mu\text{l}$  and  $20\text{-}200\mu\text{l}$  respectively, the required amount of water was extracted and deposited into Eppendorf tubes of 1.5ml. The error on the pipette was stated to be  $0.05\mu\text{l}$ . A new pipette tip was used every time a new substance was introduced. The required amount of nanoparticles were deposited into the Eppendorf tube to complete the  $1000\mu\text{l}$  of solution. To ensure all the nanoparticles were deposited into the solution, the pipette was clicked while in the solution to expel any remaining nanoparticles in the pipette tip into the solution. The Eppendorf tube was labelled with the magnetic nanoparticle size and concentration and placed into an SLS Lab Basics, 220-240V 44W Output 50-60Hz 0.4A vortexer for about 10 seconds to ensure homogeneity of the solution. This method was repeated for 20, 40, 50 and  $80\mu\text{g}/\text{ml}$  concentrations for each Zinc Ferrite and Iron Oxide nanoparticles. A letter of the alphabet was assigned to each nanoparticle-concentration pair for ease of reference in labelling the membranes and storing data.

Once the solutions were produced, the membranes were prepared for nanoparticle loading. Membranes were cut into  $2\text{x}3\text{cm}$  sheets, labelled with the correct letter of concentration and using a pipette,  $50\mu\text{l}$  of solution was deposited onto each membrane sheet. The membranes were then left to dry, to ensure that no unnecessary particles remained and the particles were fixed onto the surface. In this experiment, membranes were dried in 2 different ways, overnight in a dry, dark environment to dry at room temperature, and in a  $55^\circ\text{C}$  oven for 30 minutes. The preparation in which the membranes were heated in the oven for 30 minutes was implemented to reduce the time spent on membrane preparation. From the results, no tangible difference was observed between the 2 drying methods, only that more nanoparticles may have remained closer to the surface when dried in the oven and more may have sunk deeper into the membrane when dried overnight. This however did not affect the readings when the membranes were exposed to the laser.

$50\mu\text{l}$  of solution of three types of nanoparticles known to absorb our particular laser wavelength were also deposited onto our blue and yellow membranes. These nanoparticles were Gold Nanorods with plasmon absorption peak at 780nm, Gold Nanorods with plasmon absorption peak at 615nm and Gold Nanostars with absorption peak at 780nm. The 780nm Gold NanoStars had diameter  $60 \pm 15$  nm, 615nm Gold Nanorods had dimensions  $30 \pm 2$  nm length and  $16 \pm 1$  nm thickness, and 780nm Gold NanoRods had dimensions  $57 \pm 7$  nm length and  $16 \pm 1$  nm thickness.

These membranes were labelled separately to the alphabetised concentrations. Two control membranes were also prepared, one blue and one yellow membrane with no nanoparticles deposited.

There were some possible errors incurred in this method. Some solution was unavoidably left in pipette after transferring of each substance so the quantity of both nanoparticles and

water was unlikely to be exactly correct. There was also likely human error on the volumes of solutions as the pipetting was done in stages and some stages could have been accidentally missed or miscounted. Parallax error on the pipette was another source of uncertainty, as well as air bubbles in the pipette and extra drops of nanoparticle or water on the outside of the pipette.

### 4.3 Experimental Setup

A class 3B 780nm laser with theoretical output power 40mW was mounted on a flat platform with mounting holes specialised for optical studies. The laser was set incident on a sample holder which was able to hold thin sheets - either thermochromic or membrane. The alignment ensured that the surface of the rectangular membrane piece held by the sample holder was perpendicular to the laser beam emitted, and the centre of the membrane piece where usually the nanoparticles would be deposited was hit by the laser beam.

To analyse the change in temperature of the laser heated membranes, a Testo Ltd. 875-1i-InfraredCamera with SuperRespolution was used. The thermal imager was placed carefully in an angular position relative to the laser beam to avoid possible damages could be brought to the camera by the high intensity laser beam. The thermal imager was initially held by a human operator but was later mounted on a tripod at the edge of the platform to operate to avoid uncertainties introduced by hand movement. It was imperative that the distance between the membrane and laser was kept constant. A Tech Spin laser diode controller was used to control the intensity of a laser beam, as the output power of the laser initially fluctuated dramatically. This diode controller was essentially a semi-transparent mirror for attenuating the laser power. This was mounted along the line of propagation of the laser beam. An illustrative graph of this setup is as shown in Fig. 4.1 below.

### 4.4 Experimental Method: Membrane Laser Exposure

After membrane synthesis was completed, the membranes were mounted onto our sample holder as shown in Fig. 4.1. The output power of the laser was tested with a THOR LABS PM100D Optical Power and Energy Meter before every measurement and was shown to be averagely  $31\text{mW}/\text{cm}^2$ , with a fluctuation of around 5mW. This fluctuation was particularly prevalent at times close to when the laser was initially turned on, and seemed to take a small amount of time to ‘warm up’ and reach full power. After about one hour of so the fluctuations significantly decreased, and after around 6 hours of measurement the laser began increasing higher than 31mW to around 33mW consistently. To combat this effect the laser was first turned on and left operating for 5 minutes before being used to heat the membrane. This allowed the laser functions to be stabilized and thus uncertainties due to laser intensity fluctuations over short run times could be reduced.

Preliminary tests were conducted with gold NanoRods with absorption wavelength 615nm and 780nm and NanoStars of absorption wavelength of 780nm. These wavelengths were within the frequency range of the laser and so these values were used as the control as a specimen

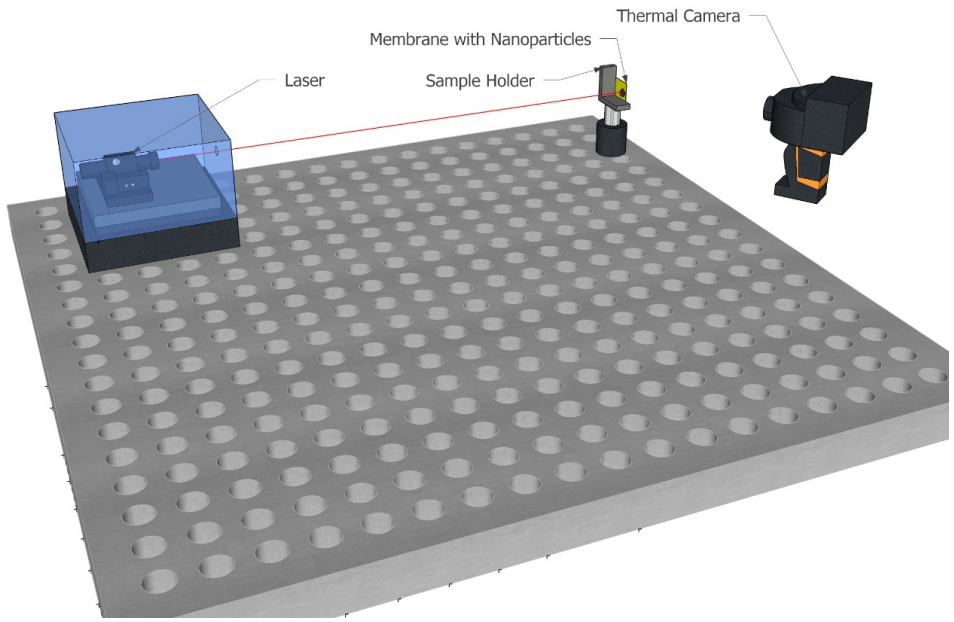


Figure 4.1: Experimental set up for measurement of increase in temperature of magnetic nanoparticles deposited onto a membrane when exposed to a laser.

for a strong positive result. In addition, NanoStars and NanoRods were selected since their larger surface area to volume ratio than the standard 0D spherical nanoparticles means they heat more efficiently. However this larger surface area causes the effect of aggregation is more profound [39].

Initial test runs to ensure that nanoparticles were correctly heating were performed for small Iron Oxide nanoparticles at  $50\mu\text{g}/\text{ml}$  concentration on a blue membrane. This was compared to results of a control membrane. The initial temperature of each subject was  $23.7^\circ\text{C}$ . The nanoparticle membrane temperature increased from this ambient temperature to around  $45^\circ\text{C}$  after approximately 2 minutes of being exposed to the laser. The control membrane was exposed to the laser for 6 minutes and showed a temperature increase of only  $0.4^\circ\text{C}$ , thus our concept that a membrane with magnetic nanoparticles deposited onto it would heat more than one without was proved.

The following tests aimed to prove the limit of detection of each nanoparticle - the lowest concentration at which a temperature change of the membrane could be seen compared to one which contained no nanoparticles.

Thermochromic sheets were used to measure temperature change qualitatively for the next set of results. A  $30 - 35^\circ\text{C}$  temperature range thermochromic sheet was attached to the back of the chosen membrane with sticky tape. This membrane-sheet pair was mounted on the source holder such that the membrane was facing the laser. The laser was turned on such that its position could be seen, and it could be ensured that the laser was in fact incident on the nanoparticle region of the membrane as shown in Fig. 4.2 below. The output power of the laser

was again recorded before every measurement. The laser was then turned on for 5 minutes, and the colour change of the thermochromic sheet was observed. If there was a very clear colour change after a short amount of time, the thermochromic sheet should have been changed to one with a higher range of activation, and if there was no change after a significant amount of time, the sheet altered to one with a lower range. This was repeated until no colour change was observed, and this range was assumed to be the excitation temperature of the nanoparticles. The results of this experiment can be seen in 5.

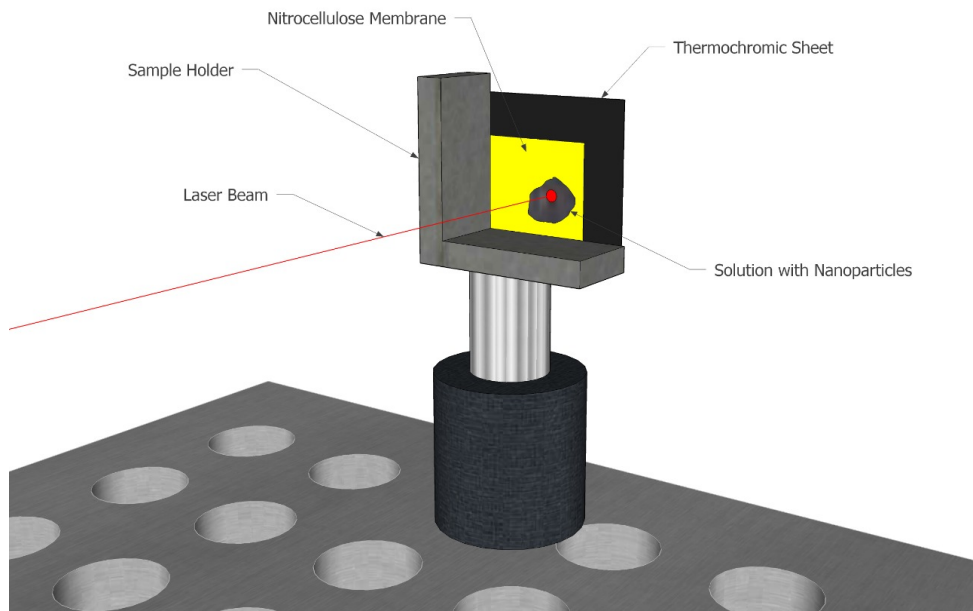


Figure 4.2: Alignment of mounted magnetic nanoparticles deposited onto a nitrocellulose membrane with a laser.

The next experimental run was performed in the absence of thermochromic sheets. The same experimental method was used, with the run time set to 15 minutes and a thermal camera image taken every minute. These results showed a straight line trend with temperature readings being around the same for each time of recording, therefore it was inferred that a far shorter run time could be used for subsequent readings. As the temperature changes from these results were significant, it was decided that in the final session of results there should be 3 new concentrations of nanoparticles (5, 10 and 15  $\mu\text{g}/\text{ml}$ ) included which were lower than the ones tested before to investigate the limit of detection further. These results were recorded over 3 minutes for each membrane, with thermal images being taken every 30 seconds.

# Chapter 5

## Discussion

by Grace Hymas, Sean MacBride, and Ivan Popov

### 5.1 Data Analysis

Code for the below described data analysis methods can be found in appendix 8.1.1. Results for each membrane colour and particle size were normalised by subtracting the control temperature at each time from nanoparticle membrane temperature. The resulting temperatures were then plotted as a function of time for each concentration measured. Uncertainties in individual temperatures were taken to be  $\pm 2^\circ\text{C}$  from the thermal camera manual, and uncertainties in the average temperature values were found by the standard deviations of the data points given by the numpy function `numpy.std` and 5.1

$$s = \sqrt{\frac{1}{N-1} \sum_{i=1}^N (x_i - \bar{x})^2} \quad (5.1)$$

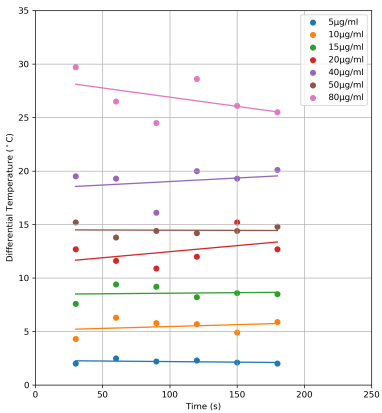
where  $N$  is the number of data points present,  $x_i$  are the individual mean temperature data points and  $\bar{x}$  is the mean of the data points.

We first investigated the change in nanoparticle membrane temperature with time relative to the concentration of nanoparticles on the membrane. It was assumed that the correlation between nanoparticle membrane temperature and time was linear and so least squares line of best fit was plotted using the `scipy.stats.linregress` function which utilises the following formulae to find intercept  $c$  and gradient  $m$  using (5.2) and (5.3).

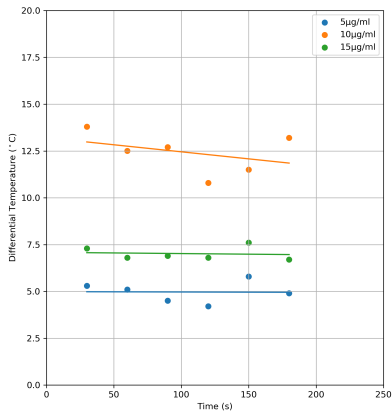
$$c = \frac{\sum_i w_i x_i^2 \sum_i w_i y_i - \sum_i w_i x_i \sum_i w_i x_i y_i}{\Delta'} \quad (5.2)$$

$$m = \frac{\sum_i w_i \sum_i w_i x_i y_i - \sum_i w_i x_i \sum_i w_i y_i}{\Delta'} \quad (5.3)$$

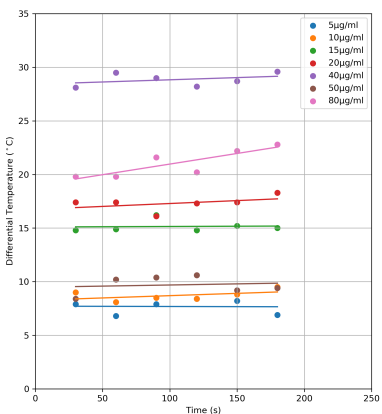
where  $\Delta' = \sum_i w_i \sum_i w_i x_i^2 - (\sum_i w_i x_i)^2$  and  $x_i$  and  $y_i$  are the differential temperatures and time data points respectively.



(a) Small Iron Oxide Nanoparticles on a Yellow Membrane



(b) Small Iron Oxide Nanoparticles on a Blue Membrane



(c) Large Iron Oxide Nanoparticles on a Yellow Membrane

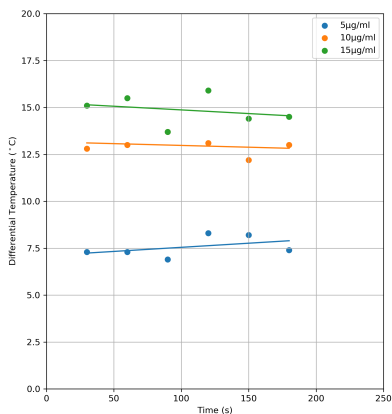


Figure 5.1: Plotted results of change in temperature against time for a series of concentrations of Iron Oxide nanoparticles exposed to a laser on different coloured nitrocellulose membranes.

## Iron Oxide Time Series Graphs

In theory, a higher concentration of nanoparticles should cause a greater increase in temperature when exposed to a laser [8]. However, this only holds true for graph in Figure 5.1a. For Figure 5.1b this assumption almost completely breaks down, with only the lower two concentrations being correctly positioned. Most significantly the  $50\mu\text{g}/\text{ml}$  specimen has a mean temperature far lower than expected, at almost  $20^\circ\text{C}$  below the average temperature for the  $40\mu\text{g}/\text{ml}$  concentration. Figure 5.1c shows a similar trend, with our  $15\mu\text{g}/\text{ml}$  average temperature being located at nearly half the temperature of the  $10\mu\text{g}/\text{ml}$  result. Figure 5.1d, is close to being as expected, with only the  $50\mu\text{g}/\text{ml}$  concentration being placed strangely according to prior knowledge. It is a possible conclusion at this stage that perhaps the concentrations were made incorrectly, and they are not in fact the concentrations expected.

The linear trends of 5.1a-5.1d most frequently show a constant differential temperature with respect to time. Deviations from this seem to be random, and most likely due to random uncertainties as both positive and negative correlation changes can be seen with equal frequency.

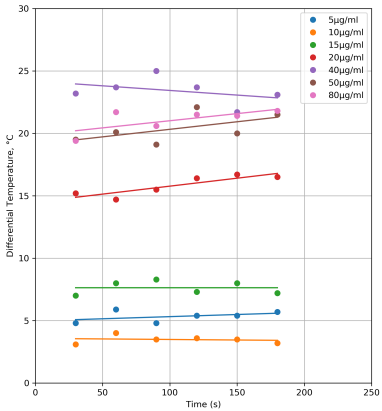
## Zinc Ferrite Time Series Graphs

Initially it was expected that differential temperature curve with time would undergo a rapid increase and then become more shallow with time. However, the experimental data does not show any increase in temperature, instead the temperature readings are fluctuating. Since the data measurements were taken with 30 s intervals, the rapid increase in temperature is therefore expected to happen during the first 30 s of the exposure to the laser. Results for 5.2b and 5.2d show the expected increase in mean temperature with concentration here. 5.2c shows an almost correct increase in mean temperature with concentration increase, with the significant outlier being the  $80\mu\text{g}/\text{ml}$  concentration which shows a temperature roughly around the mean temperature of the  $20\mu\text{g}/\text{ml}$  zinc ferrite concentration. This concentration should be treated as an anomaly and removed. 5.2a shows a confusing trend similar to that seen for some of the graphs of Iron Oxide nanoparticle changes in mean temperature with time, in that a few concentrations seem to be randomly ordered and not showing a trend. Similarly, it could be suggested that the concentrations here are incorrectly assumed.

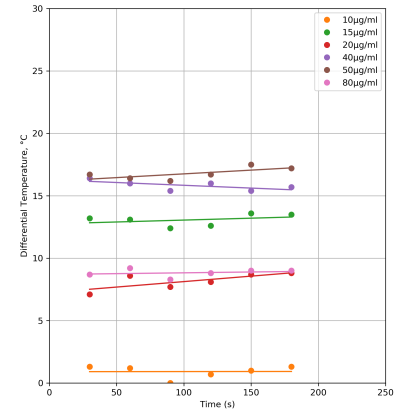
## Membrane Color

To investigate the effect of different coloured membranes on our nanoparticle temperatures, graphs of results of mean temperature for the nanoparticles deposited onto the blue membranes minus the temperature for yellow membranes were plotted against time for both nanoparticle types in figure 5.3.

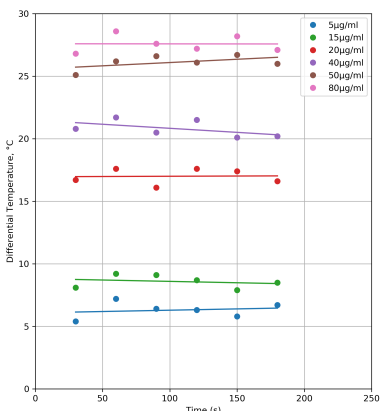
Iron Oxide nanoparticle results shown in 5.3a seem to imply mixed conclusions. We seem to see 3 trends of the mean temperature for the blue membrane being higher ( $10\mu\text{g}/\text{ml}$  small,  $10\mu\text{g}/\text{ml}$  large and  $5\mu\text{g}/\text{ml}$  small), 2 trends of the mean temperature for the yellow membrane being roughly around zero ( $5\mu\text{g}/\text{ml}$  large and  $15\mu\text{g}/\text{ml}$  large) - albeit with large fluctuations for the  $15\mu\text{g}/\text{ml}$  large result, and one result showing a higher temperature for the yellow membrane



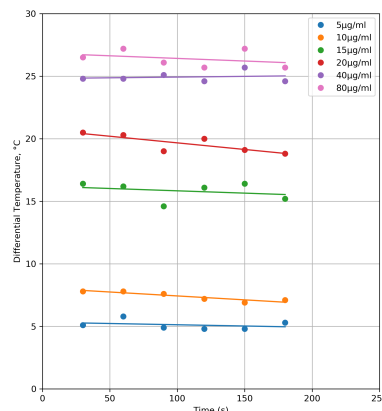
(a) Small Zinc Ferrite Nanoparticles on a Yellow Membrane



(b) Small Zinc Ferrite Nanoparticles on a Blue Membrane

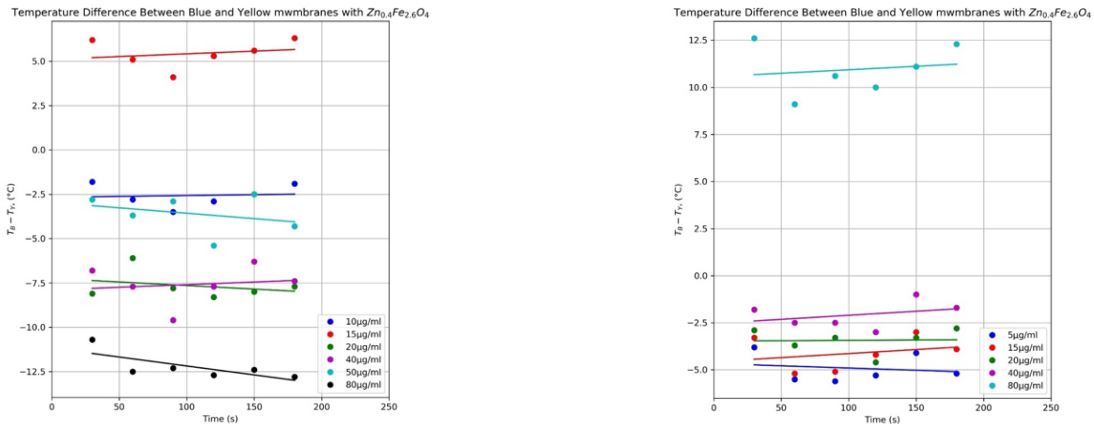


(c) Large Zinc Ferrite Nanoparticles on a Yellow Membrane



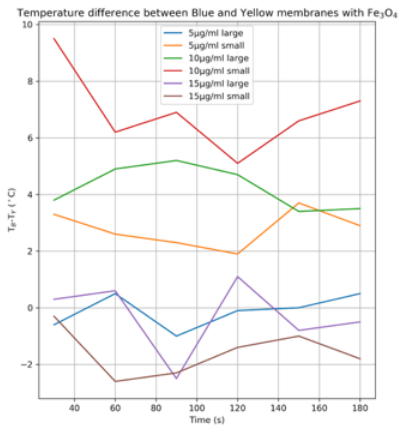
(d) Large Zinc Ferrite Nanoparticles on a Blue Membrane

Figure 5.2: Plotted results of change in temperature against time for a series of concentrations of Zinc Ferrite nanoparticles exposed to a laser on different coloured nitrocellulose membranes.



(a) Temperature difference for Small Zinc Ferrite nanoparticles on Different Membranes

(b) Temperature difference for Large Zinc Ferrite nanoparticles on Different Membranes



(c) Temperature difference for Iron Oxide nanoparticles on Different Membranes

Figure 5.3: Temperature differences for nanoparticles on different colored membranes

(15 µg/ml small). There seems to be no correlation between large and small particles and concentrations from this data, implying that the nanoparticle size or concentration are not dependant on the membrane colour, but this fluctuation is stochastic.

5.3b shows perhaps one of the most significant trends yet, with a clear larger temperature being seen for all concentrations deposited onto a yellow membrane. This data set also shows a significant outlier at 80 µg/ml for unclear reasons.

5.3c shows again an extremely significant trend, and one which is the same as what is shown in 5.3b. These results show clearly that the blue membrane absorbs more energy than the yellow one, which is in contradiction to previous results, although said previous results are arguably weaker in possibility.

## 5.2 Limit of Detection

The limit of detection is defined as the lowest concentration that can be detected due to a temperature change of the nanoparticles on the membrane. In order to find our limit of detection we must plot graphs of mean temperature change of each nanoparticle relative to its concentration, plot a line of best fit and extrapolate this line of best fit to where there is zero mean temperature change. However the type of correlation of these data points was unclear, and therefore three types of lines of best fit were analysed, with results discussed starting at 5.2.1.

Since the uncertainty of the individual temperature readings is  $\pm 2^\circ\text{C}$ , all of the readings that are less or equal to  $2^\circ\text{C}$  cannot be used to determine whether there are nanoparticles in the solution. The limit of detection is therefore determined by the resolution of the thermal camera.

The uncertainties in the concentration of nanoparticles in the solution were found by assuming two situations: when there is the maximum possible amount of nanoparticle concentrate with the minimum possible amount of water for the upper boundary and vice versa for the bottom boundary. The absolute uncertainty was found to be  $\pm 0.5\mu\text{g}/\text{ml}$ . The percentage uncertainty is high for  $5\mu\text{g}/\text{ml}$  solution, as it reaches 10%, however, as the concentration increases, the percentage uncertainty becomes  $< 1\%$  and no longer significantly affects the results.

The uncertainties on the lines of best fit were estimated via a chi-squared fit of the curves relative to the data points with the Python function `scipy.stats.chisquare` which utilises the formula 5.4 [40].

$$\chi^2 = \sum_{i=1}^n \frac{(O_i - E_i)^2}{E_i} \quad (5.4)$$

This formula predicts the goodness of fit of a line to a set of data points, and therefore was intended for use as deciding which fit is most accurate to our trends, as well as giving a rough idea of uncertainty to lines for which uncertainties could not be calculated.

Reduced-chi squared shows us more clearly how good the model fit is, as it standardises the data. A  $\chi >> 1$  indicates a poor model fit. A  $\chi > 1$  indicates that the fit has not fully captured the data, or that error variance has been underestimated. A  $\chi = 1$  tells us that the observations and error estimations are in agreement and therefore the fit is ideal, and a  $\chi < 1$  indicates an overfitted model; one which has either fitted noise as if it was a trend shown by the model itself or where the errors have been overestimated.

We also calculate the chi squared probability, which is also outputted from the above-mentioned Python function. This probability tells us how likely the fit is to be significant, with this particular function outputting a low value indicating that the fit is likely to be bad, and a high value indicating a good fit. A chi-squared probability greater than 0.95 is said to be extremely statistically significant, with there being a strong relationship between the models of our lines of best fit and our experimental data points. Please note that usually the significance is opposite for high and low p values, but in this case the function outputs one minus the probability.

### 5.2.1 Linear Trend

It was initially assumed that the correlation between nanoparticle membrane temperature and concentration was linear and so least squares line of best fit was plotted using the `scipy.stats.linregress` function which utilises 5.2 and 5.3 to find intercept  $c$  and gradient  $m$ .

The uncertainties in intercept  $\alpha_c$  and gradient  $\alpha_m$  are given by equations 5.2.1 and 5.6.

$$\alpha_c = \sqrt{\frac{\sum_{i=1}^N w_i x_i^2}{\Delta'}}$$

(5.5)

$$\alpha_m = \sqrt{\frac{\sum_{i=1}^N w_i}{\Delta'}} \quad (5.6)$$

where  $\Delta' = \sum_i w_i \sum_i w_i x_i^2 - (\sum_i w_i x_i)^2$  and  $x_i$  and  $y_i$  are the differential temperatures and time data points respectively.

### Iron Oxide Nanoparticles

Figure 5.4 shows a significant difference between variation in mean temperature with increasing concentration when either blue or yellow membranes are used. For the small sized iron oxide nanoparticles we seem to see a similar gradient present for both yellow and blue membranes, but a roughly 5°C increase in mean temperature of the blue membrane line for the same concentrations. This suggests that the yellow membrane could be absorbing far more of the laser energy. For the large iron oxide particles, we can see a radically different gradient. Mean temperature seems to increase far more dramatically per unit concentration for the blue membrane. It is possible that the large iron oxide particles on the blue membrane is an outlier due to this radically different gradient. We can see a difference in mean temperature of the lines again, except in this case our blue membrane reading is lower. It is thus inconclusive to say if one membrane absorbs better than another.

Table 5.1 summarizes the limits of detection and chi squared fits. We can see that all of our concentration limits are negative, rendering them unphysical and therefore inconclusive on what the limit of detection for these nanoparticles are.

### Zinc Ferrite Nanoparticles

Taking the small Zinc Ferrite nanoparticle results, we can see a fairly large difference in gradients between the two colours of membranes, with the blue membrane mean temperatures increasing more rapidly with concentration than the yellow membrane results. The yellow membrane temperatures seem higher for lower concentrations, and lower than blue for higher concentrations, with an equilibrium reached at roughly 40 $\mu\text{g}/\text{ml}$ . The gradients and therefore changes in mean temperature with increasing time for the large nanoparticles are remarkably close and noticeably similar to the blue membrane large particle results - perhaps suggesting that the small yellow

Particle Size	Small		Small	
Membrane color	Yellow	Blue	Yellow	Blue
Limit Of Detection ( $\mu\text{g/ml}$ )	-12 $\pm$ 7	-30 $\pm$ 114	-78 $\pm$ 69	-6 $\pm$ 2
Chi Square	4.5	3.4	16.5	0.2
Reduced Chi Square	0.8	1.7	2.7	0.09
Chi Square Probability	0.6	0.2	0.01	0.9

Table 5.1: Statistical significance of a least squares linear fit fitted to experimental data of change in mean temperature of Iron Oxide nanoparticles when exposed to a laser relative to their varying concentration.

membrane results may be outliers. We can see here that the blue membrane results are constantly around 3°C higher than the yellow membrane results, suggesting, given that the Iron Oxide results showed both versions of the trend, that this one is likely to be correct and that yellow membranes absorb more energy from the laser. Again, it is significant that the error estimated on both mean temperature and concentration is far too small, as only a few data points fall on the line of best fit within their uncertainties.

Particle Size	Small		Small	
Membrane color	Yellow	Blue	Yellow	Blue
Limit Of Detection ( $\mu\text{g/ml}$ )	-24 $\pm$ 15	-103 $\pm$ 153	-25 $\pm$ 11	2 $\pm$ 3
Chi Square	10.6	15.2	3.9	3.5
Reduced Chi Square	2.7	5.1	1.3	1.2
Chi Square Probability	0.03	0.002	0.3	0.3

Table 5.2: Statistical significance of a least squares linear fit fitted to experimental data of change in mean temperature of Zinc Ferrite nanoparticles when exposed to a laser relative to their varying concentration.

Our chi-squared probability values are mostly constantly low here, indicating a bad fit. This is especially true for our small nanoparticles deposited onto a blue membrane. All chi-squared values lie above one, indicating that the null hypothesis that the line of best fit does fit the data should be rejected. The small nanoparticle values indicate a bad fit as they are much greater than one, and the large nanoparticle values show that the fit has not fully captured the trend of the data.

	Outlier Included Fit		Outlier Removed Fit	
Membrane color	Yellow	Blue	Yellow	Blue
Particle Size	Small	Big	Small	Big
Limit Of Detection ( $\mu\text{g}/\text{ml}$ )	3.5	1.7	3.8	2.9
Chi Square	6.2	11.8	1.7	6.8
Reduced Chi Square	1.0	2.0	0.3	1.4
Chi Square Probability	0.4	0.07	0.9	0.2

Table 5.3: Statistical significance of a logarithmic fit fitted to experimental data of change in mean temperature of Iron Oxide nanoparticles when exposed to a laser relative to their varying concentration.

### 5.2.2 Logarithmic Trend

On closer inspection of the data points and after significant non-physical limit of detection values, a logarithmic fit was attempted. The data was re plotted using the `scipy` function `scipy.optimize.curvefit` on Python and was optimised using equation 5.7.

$$y = a \ln bx + c \quad (5.7)$$

#### Iron Oxide Nanoparticles

Unfortunately for this fit our blue membrane results had to be excluded as there was too few data points to plot this particular fit for it to be significant. Our data shows the expected positive correlation trend, with the large Iron Oxide nanoparticles heating initially at a greater rate than the smaller ones, and always being located at a greater mean temperature than them. Our limits of detection for this line of best fit are positive and therefore physical, indicating that this is perhaps a better fit than our linear assumption.

Chi squared probability for our large yellow particles is significantly low, indicating a very bad fit to the data points. This is mostly likely due to the variance in the large nanoparticle data. The reduced chi square value is much greater than one, indicating an incorrect fit. It is usual that our chi squared probability is exactly one for our small nanoparticles deposited onto our membrane. This indicates the best fit possible, which is not reflected by the probability, or much by the visual implications of the graph. It is an interesting point here that the data points seem to diverge more at higher concentrations, which indicates that the effect causing our errors is more significant for higher temperatures also.

Outliers are far clearer here, and therefore it was decided that a fit should be attempted with outliers excluded from the data. This fit is shown in Fig. 5.6b, with the grey data points being the removed points.

The outlier removed results can be seen in table 5.3. Interestingly our limits of detection

are increased, as well as the chi square probability. For our small iron oxide nanoparticles our probability is extremely close to one which could mean that our limit of detection for small iron oxide particles on a yellow membrane is likely close to  $3.8 \mu\text{g/ml}$ . This being said, our reduced chi squared value is close to zero indicating the possibility of overfitting.

### Zinc Ferrite Nanoparticles

This fit again gives positive concentration values which indicates that it is perhaps more appropriate. Large and small nanoparticles for each coloured membrane are above and below each other respectively as expected, as large nanoparticles will heat up more per unit concentration than small ones. Blue membrane nanoparticle temperatures seem to lie below yellow membrane values for their respective data pairs, indicating that the blue membranes are absorbing more of the laser wavelength here. We can see a particularly bad fit for the small nanoparticles on the blue membrane which is reflected in its very large reduced chi square value.

We have an extremely small value of chi squared probability for our small yellow data, along with a very high reduced chi square value. The reason for this is unclear, as it seems a better fit than some other curves. Large nanoparticle reduced chi squared values seem very good, although probability is low, most likely due to significant data outliers. With this considered, outliers were removed again and the results are shown below in fig 5.7b and table 5.4.

Particle Size	Small		Large	
Membrane color	Yellow	Blue	Yellow	Blue
Limit Of Detection ( $\mu\text{g/ml}$ )	4.1	0.3	3.4	6.0
Chi Square	18.5	13.8	4.5	4.2
Reduced Chi Square	3.1	2.8	0.9	0.8
Chi Square Probability	0.005	0.02	0.5	0.5

Table 5.4: Statistical significance of a logarithmic fit fitted to experimental data of change in mean temperature of Zinc Ferrite nanoparticles when exposed to a laser relative to their varying concentration.

Our blue membrane data produces the only changed fits here. We can see a significant increase in chi squared probability for both, as well as reduced chi squared values tending closer to one. The large blue membrane shows a particularly good result, with chi squared probability equal to one indicating a perfect fit, and reduced chi square value just under one, indicating a fairly good fit with slight underfitting, which makes sense considering the removed data points. In fact, for most chi squared values under one it is most likely due to the fact there are not many data points, and more experimental data needs to be recorded.

Limits of detection are in a good small range for this fit, ranging from  $3.4 - 5.7$ .

	Outlier Included Fit		Outlier Removed Fit	
Membrane color	Yellow			
Particle Size	Small	Big	Small	Big
Limit Of Detection ( $\mu\text{g}/\text{ml}$ )	2.0	-1.3	2.8	0.1
Chi Square	5.7	13.5	0.4	6.8
Reduced Chi Square	1.0	2.3	0.08	1.4
Chi Square Probability	0.04	0.04	0.08	0.09

Table 5.5: Statistical significance of a square root fit fitted to experimental data of change in mean temperature of Iron Oxide nanoparticles when exposed to a laser relative to their varying concentration.

### 5.2.3 Square Root Trend

Our final fit attempted was a square root trend given by the formula:

$$y = a\sqrt{bx} + c \quad (5.8)$$

where  $y$  is mean temperature data points and  $x$  are concentration data points, and  $a$   $b$  and  $c$  are the constant variables fitted by the optimisation function.

#### Iron Oxide Nanoparticles

Blue membrane data points have again been removed due to there being not enough data to fit the points, which is seen in figure 5.8b. We again see the expected positive correlation here, with large nanoparticles mean temperature lying above small for all concentrations as expected. We can see however that we have a negative limit of detection again, indicating a not good fit. This is reflected by an extremely high reduced chi square value and low chi square probability. Unusually, our reduced chi square is exactly one for our small nanoparticles, but is in complete contrast with our very low chi squared probability. Again, this is likely due to outliers, and therefore these were removed again.

Removal of outliers gives visually a much better fit, with mean temperature increasing far more per unit concentration, and both limits of detection now being physical- albeit only just about for the large nanoparticles. Chi square probability is still so low, that this fit must still be rejected for these data points. These results are detailed in table 5.5.

#### Zinc Ferrite Nanoparticles

We have a clear outlier in the fit here without blue membrane small nanoparticle data seen in figure 5.9a. This yields an extremely negative limit of detection value and should be rejected immediately. The other fits in 5.9b show our expected trends, although our large blue membrane

Outlier Included Fit				
Particle Size	Small		Large	
Membrane color	Yellow	Blue	Yellow	Blue
Limit Of Detection ( $\mu\text{g}/\text{ml}$ )	4.1	0.3	3.4	6.0
Chi Square	18.5	13.8	4.5	4.2
Reduced Chi Square	3.1	2.8	0.9	0.8
Chi Square Probability	0.005	0.02	0.5	0.5
Outlier Removed Fit				
Particle Size	Small		Large	
Membrane color	Yellow	Blue	Yellow	Blue
Limit Of Detection ( $\mu\text{g}/\text{ml}$ )	4.1	5.7	3.4	5.3
Chi Square	18.5	6.8	4.5	2.6
Reduced Chi Square	3.1	1.7	0.9	0.7
Chi Square Probability	0.005	0.14	0.5	1.0

Table 5.6: Statistical significance of a square root fit fitted to experimental data of change in mean temperature of Zinc Ferrite nanoparticles when exposed to a laser relative to their varying concentration.

data seems to increase unusually rapidly past  $40\mu\text{g}/\text{ml}$ . Probabilities for large nanoparticles are particularly good, although chi square value for blue large is negative so must be rejected. Overall, this fit cannot be said to be conclusive for these data points.

Outlier removal was performed again in table 5.6, with no real significant improvement in chi square values or probabilities, although visually the fit is improved.

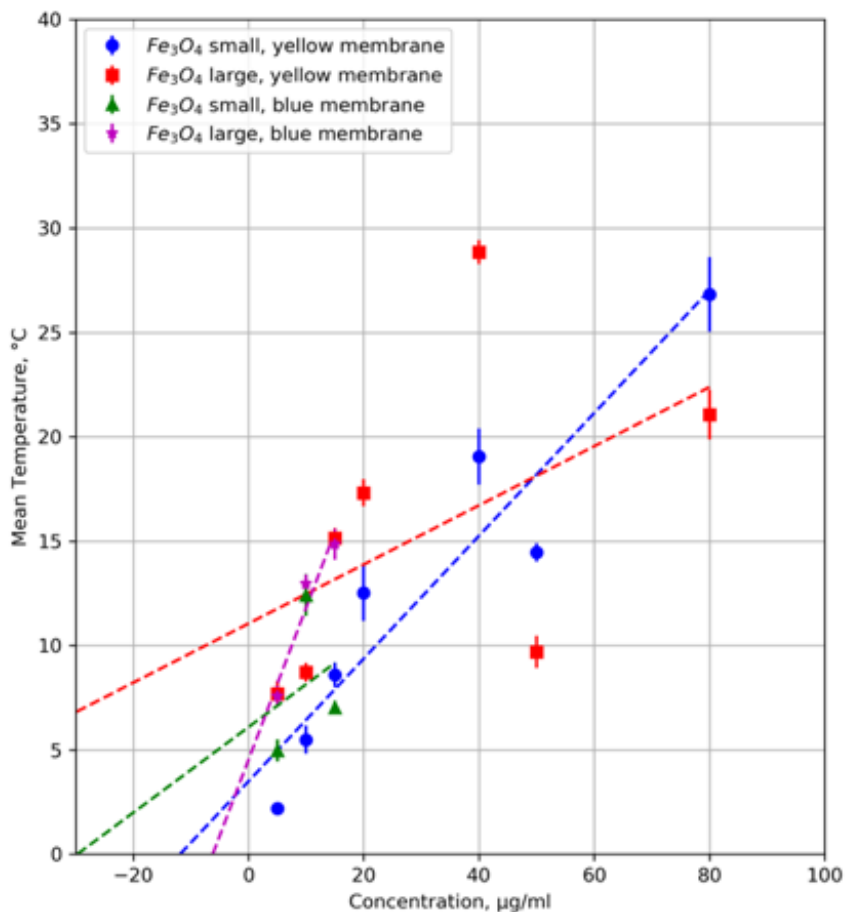


Figure 5.4: A graph of mean temperature reached by varying sizes of Iron Oxide nanoparticles on different coloured membranes against the concentration of nanoparticles present. Please note the lines of best fit are shown as extrapolated to the left past the data points to illustrate the limit of detection – the concentration at which the mean temperature tends to zero.

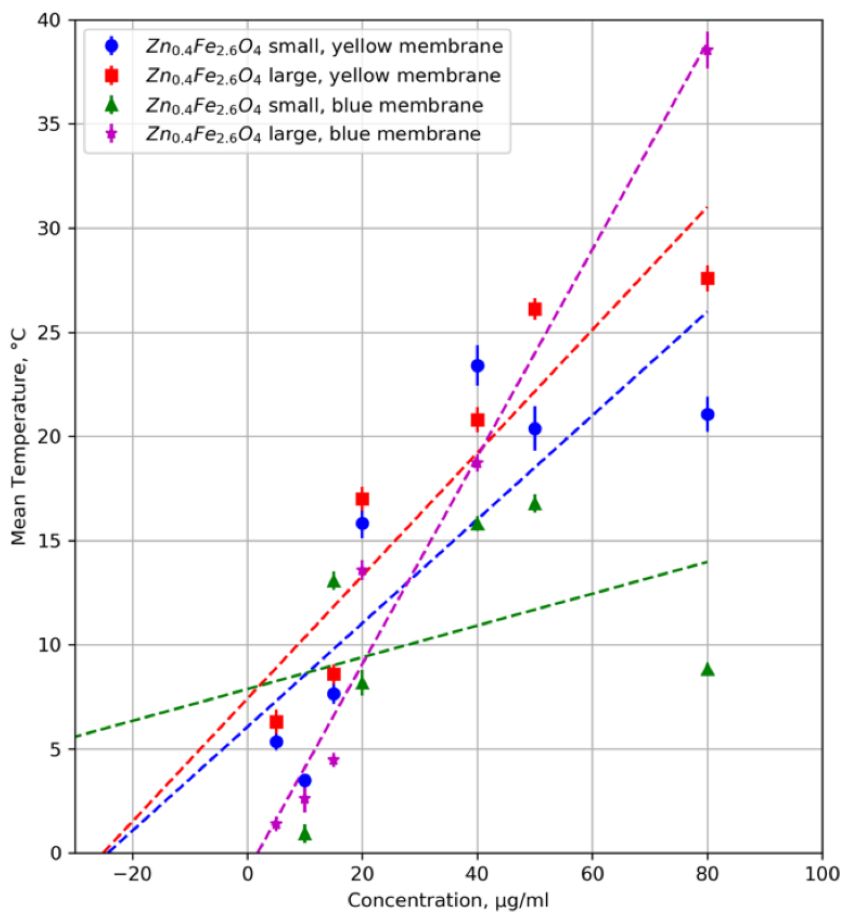
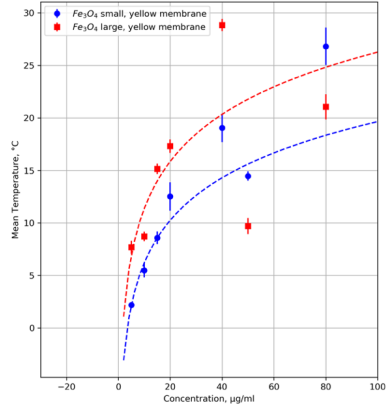
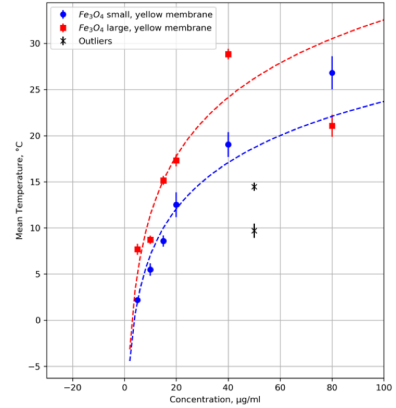


Figure 5.5: A graph of mean temperature reached by varying sizes of Zinc nanoparticles on different coloured membranes against the concentration of nanoparticles present. Please note the lines of best fit are shown as extrapolated to the left past the data points to illustrate the limit of detection – the concentration at which the mean temperature tends to zero.

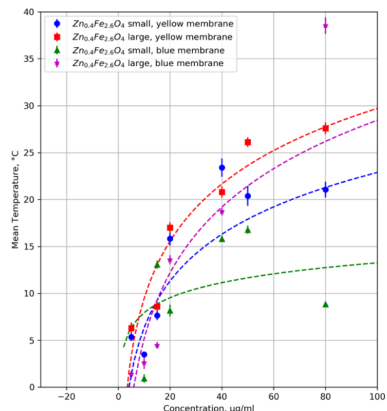


(a) Outlier included logarithmic fit

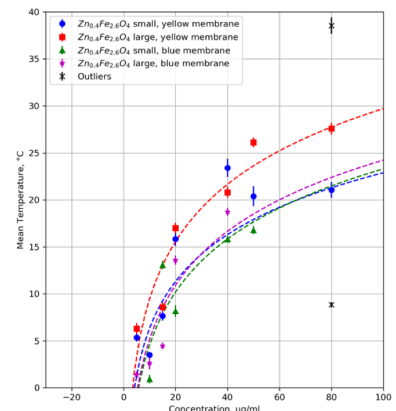


(b) Outlier removed logarithmic fit

Figure 5.6: A graph of mean temperature reached by varying sizes of Iron Oxide nanoparticles on different coloured membranes against the concentration of nanoparticles present. Outliers are included in the fit on the left, and removed for the fit on the right. They are plotted in grey on the right.

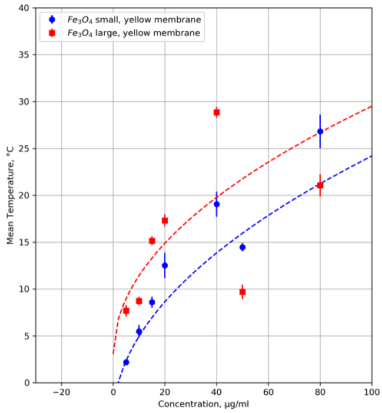


(a) Outlier included logarithmic fit

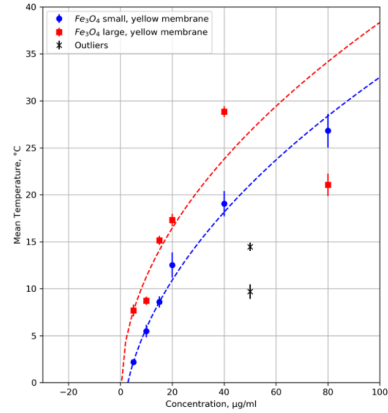


(b) Outlier removed logarithmic fit

Figure 5.7: A graph of mean temperature reached by varying sizes of Zinc Ferrite nanoparticles on different coloured membranes against the concentration of nanoparticles present. Outliers are included in the fit on the left, and removed for the fit on the right. They are plotted in grey on the right.

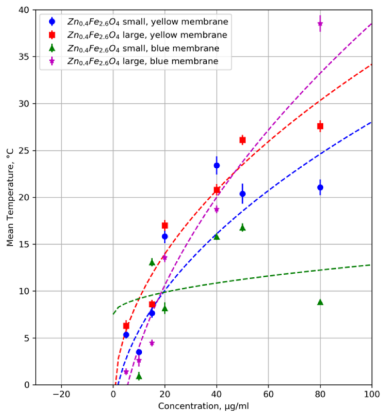


(a) Outlier included square root fit

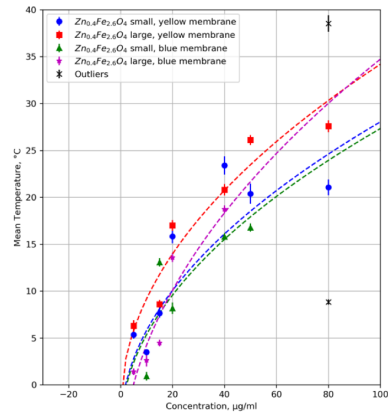


(b) Outlier removed square root fit

Figure 5.8: A graph of mean temperature reached by varying sizes of Iron Oxide nanoparticles on different coloured membranes against the concentration of nanoparticles present. Outliers are included in the fit on the left, and removed for the fit on the right. They are plotted in grey on the right.



(a) Outlier included square root fit



(b) Outlier removed square root fit

Figure 5.9: A graph of mean temperature reached by varying sizes of Zinc Ferrite nanoparticles on different coloured membranes against the concentration of nanoparticles present. Outliers are included in the fit on the left, and removed for the fit on the right. They are plotted in grey on the right.

# Chapter 6

## Conclusion

by Jennifer Lin, Anja Rellstab, Wenhao Wu

### 6.1 Summary of Findings

The initial experimental trials using only the thermochromic sheets to monitor the temperature changes showed inconclusive results regarding the correlation between the existence of nanoparticles and temperature changes. This suggests that our designed thermochromic sheet method or the type of thermochromic sheet used was not sensitive enough for investigating shifts in temperature changing rate caused by the presence of nanoparticles on membrane.

Later results obtained by deploying a thermal imager in monitoring temperature changes were analysed in two ways. Linearly fitted lines found no clear correlation between the temperature changes and the sizes of the nanoparticles or the concentrations of the Zinc Ferrite nanoparticle solutions. The differential temperature lines plotted with respect to time of being exposed to laser did not exhibit expected trends. This suggested that the concentrations of nanoparticle solutions could have been wrongly assumed.

The logarithmic fit method found that there could be a correlation between the concentration of nanoparticle solutions and the sample's temperature rising rate, but the collected data sample size was too small draw any statistically convincing conclusion on this.

Additionally, the limit of detection is defined as the lowest concentration can be detected due to a temperature change of the tested sample, the obtained results in terms of limit of detection is heavily dependent on the resolution of thermal camera, but the effect of this on the final results was normalised by the statistical approaches we adopted in data analysis.

The blue and yellow membranes were believed to have different heat absorption abilities due to the colour of them and the different pore sizes. Due to heat capacity values, It was in principle that the blue membrane with smaller pore size, which can hold more air, should be absorbing more heat than the yellow membrane, but our data showed no clear results in terms of which membrane absorbs more heat under roughly the same conditions.

## 6.2 Improvement of Findings

The way that the solution was deposited on the membrane was not standardised. We have just dropped the solution from the pipette onto the membrane. There was no control of the shape of the solution drop when it was drying. Therefore the distribution of the nanoparticles on the surface of the membrane may not be homogeneous. This explains why the temperature of the 80  $\mu\text{g}/\text{ml}$  is much lower than expected. The laser may be irradiating the area where the concentration of nanoparticles is lower than 80  $\mu\text{g}/\text{ml}$ .

In order to avoid a situation like this in the future, the deposition of the solution must be standardised. The plastic form of circular shape will be placed on top of the membrane and the solution will be deposited inside the form. Then the solution will be left to dry and only after that the form will be removed. This way of depositing the solution guarantees the same surface for all nanoparticle concentrations and therefore makes the distribution of nanoparticles on the membrane more homogeneous.

Our least squares line of best fit is arguably a large reason why limits of detection are impossibly below zero. A least squares line of best fit is particularly susceptible to outlying data points, as it attempts to minimise the weights of all data points. As it is clear there are significant outliers in our data, it may be beneficial to use another type of regression fit in the future, for example Ridge or LASSO regression, which both minimise weights of data points that seem to deviate greatly from the expected model.

## 6.3 Evaluation of project

Logistically, there were some issues acquiring the necessary materials and equipment, such as delays with the membrane supplier and no suitable lasers available. The laser used had a significantly lower output than previously anticipated however this did not cause major issues to the experiment. Due to these unforeseen setbacks, data collection only began a couple of weeks into the project which resulted in insufficient evidence to draw any concrete conclusions.

Overall, the results largely followed the expected trend of increasing temperatures with concentrations, although there were several anomalies hence more experimental results should be taken in the future. With the data collected, linear, logarithmic and square root trend curves of temperature change against concentration were plotted for the various nanoparticles and membranes. The logarithmic curve seemed most favourable although further experimentation is needed before conclusive results can be made. Furthermore, more concentrations will need to be tested, to evaluate the accuracy of the extrapolated limit of detection from this experiment. As expected the temperature change was dependent on the nanoparticle size, with a larger temperature change for larger nanoparticles due to their higher absorption efficiency. Although, no definitive conclusions can be drawn, this experiment provides promising preliminary data which could potentially lead to improved sensitivity of LFAs.

Although not all the experimental aims and objectives were met, the magnetic nanoparticles were successfully deposited onto membranes of 2 different pore sizes and colors, and various concentrations of magnetic nanoparticles were tested. These membranes were then dried and

exposed to a laser which excited the nanoparticles, heating them up. An IR camera was then used to evaluate the temperature change. Limited experiments were run using thermochromic sheets as a quantitative thermal contrast tool due to time constraints. However, they seem like a promising avenue to venture in further experimentation, as thermal contrast LFAs with thermochromic sheets could potentially aid with early detection and increased sensitivity in disease diagnosis, and potentially even quantifying the severity of disease.

Given more time, calibration curves could be implemented to create an application to for reading and analysing LFAs, to provide users with a more comprehensive diagnosis as proposed in the future prospects.

## 6.4 Final Summary

The basic aim to test the sensitivity of nitrocellulose membrane in conjunction of magnetic nanoparticles and laser was met as we were able to make use of thermal imaging to investigate the temperature change of the sample after thermal activation. The data were then subsequently fitted to a logarithmic function and tested with chi-squared test for goodness of fit. However the results obtained from the experimentation was inconclusive due to the initial difficulty in acquiring the necessarily hardwares to conduct the experiment. For example, there were not enough experimental runs to fully ensure that the concentrations of the nanoparticle solutions are correctly assumed and there were also not enough experimental data to test the sensitivity of the thermochromic sheets in conjunction with the sample. [and add a few more things in the project that could be improved]

The idea of using the results from the IR camera in conjunction with an application which is capable of calculating colour calibration curve has been explored. This could be a feasible future use of integrating the quantified results of the LFAs to provide user clients qualitative informations.

# Chapter 7

## Acknowledgements

There are many people without whom this project would not have been possible and we are all extremely grateful for the time and effort you all have put into this project.

Firstly, we would like to give special thanks to the Royal Institute and University College London for sharing their resources and allowing us to carry out the experiments in their laboratories. Their willingness to provide us with the necessary equipment and help when problems arose really helped us promptly complete the experiment.

We would also like to express our greatest appreciation to our principal investigator, Professor Thanh Nguyen. Her support and guidance throughout the project was truly invaluable. In addition, her professional insight on unfamiliar scientific concepts and constructive feedback on the project approach during the consultations played a vital role in the overall progress of this project.

Last but not least, we would like to offer our utmost gratitude to Francesco Rossi, Kelvin Vine and Thithawat Trakoolwilaiwan for taking time out of their busy schedules to assist us with the experimental methods, data collection and offering up their advice over the course of the project. Their enthusiasm for the work was truly inspirational and we would like to thank them all for their constant encouragement and support.

# Bibliography

- [1] J. D. Hunter, “Matplotlib: A 2d graphics environment,” *Computing In Science & Engineering*, vol. 9, no. 3, pp. 90–95, 2007.
- [2] K. M. Koczula and A. Gallotta, “Lateral flow assays,” *Essays In Biochemistry*, vol. 60, no. 1, pp. 111–120, 2016.
- [3] M. Sánchez-Purrà, M. Carré-Camps, H. de Puig, I. Bosch, L. Gehrke, and K. Hamad-Schifferli, “Surface-enhanced raman spectroscopy-based sandwich immunoassays for multiplexed detection of zika and dengue viral biomarkers,” *ACS Infectious Diseases*, vol. 3, no. 10, pp. 767–776, 2017.
- [4] K. D. Jones, “Troubleshooting protein binding in nitrocellulose membranes, part 1: Principles,” *IVD Technologies*, vol. 5, no. 2, pp. 32–41, 1999.
- [5] Q. Li, H. Qi, Z. Zhong, H.-X. Zhou, C.-Y. Deng, H. Zhu, J.-F. Li, and X.-L. Wang, “A rapid and highly sensitive protocol for the detection of escherichia coli o157:h7 based on immunochromatography assay combined with the enrichment technique of immunomagnetic nanoparticles,” *International Journal of Nanomedicine*, p. 3033, 2011.
- [6] S. Workman, S. K. Wells, C.-P. Pau, S. M. Owen, X. F. Dong, R. LaBorde, and T. C. Granade, “Rapid detection of hiv-1 p24 antigen using magnetic immuno-chromatography (mict),” *Journal of Virological Methods*, vol. 160, no. 1-2, pp. 14–21, 2009.
- [7] S. Rong-Hwa, T. Shiao-Shek, C. Der-Jiang, and H. Yao-Wen, “Gold nanoparticle-based lateral flow assay for detection of staphylococcal enterotoxin b,” *Food Chemistry*, vol. 118, no. 2, pp. 462–466, 2010.
- [8] Z. Qin, W. C. W. Chan, D. R. Boulware, T. Akkin, E. K. Butler, and J. C. Bischof, “Significantly improved analytical sensitivity of lateral flow immunoassays by using thermal contrast,” *Angewandte Chemie International Edition*, vol. 51, no. 18, pp. 4358–4361, 2012.
- [9] A. E. Urusov, M. K. Gubaidullina, A. V. Petrakova, A. V. Zherdev, and B. B. Dzantiev, “A new kind of highly sensitive competitive lateral flow immunoassay displaying direct analyte-signal dependence. application to the determination of the mycotoxin deoxynivalenol,” *Micromochimica Acta*, vol. 185, no. 1, 2017.

- [10] D. R. Hristov, C. Rodriguez-Quijada, J. Gomez-Marquez, and K. Hamad-Schifferli, “Designing paper-based immunoassays for biomedical applications,” *Sensors*, vol. 19, no. 3, 2019. [Online]. Available: <http://www.mdpi.com/1424-8220/19/3/554>
- [11] M. ELSHAL and J. MCCOY, “Multiplex bead array assays: Performance evaluation and comparison of sensitivity to elisa,” *Methods*, vol. 38, no. 4, pp. 317–323, 2006.
- [12] S. X. Leng, J. E. McElhaney, J. D. Walston, D. Xie, N. S. Fedarko, and G. A. Kuchel, “Elisa and multiplex technologies for cytokine measurement in inflammation and aging research,” *The Journals of Gerontology Series A: Biological Sciences and Medical Sciences*, vol. 63, no. 8, pp. 879–884, 2008.
- [13] K. Mohd Hanafiah, N. Arifin, Y. Bustami, R. Noordin, M. Garcia, and D. Anderson, “Development of multiplexed infectious disease lateral flow assays: Challenges and opportunities,” *Diagnostics*, vol. 7, no. 3, p. 51, 2017.
- [14] H. Shamloo Ahmadi, M. Heiat, H. Rashedi, and A. Latifi, 2015. [Online]. Available: [http://www.biotechrep.ir/article\\_69167\\_21d318e6573b7563d30ad754cff7dd3f.pdf](http://www.biotechrep.ir/article_69167_21d318e6573b7563d30ad754cff7dd3f.pdf)
- [15] M. Corporation, “Rapid lateral flow test strips,” 2002. [Online]. Available: [https://www.emdmillipore.com/Web-US-Site/en\\_CA/-/USD/ShowDocument-Pronet?id=201306.12550](https://www.emdmillipore.com/Web-US-Site/en_CA/-/USD/ShowDocument-Pronet?id=201306.12550)
- [16] L. H. Mujawar, A. A. Maan, M. K. I. Khan, W. Norde, and A. van Amerongen, “Distribution of biomolecules in porous nitrocellulose membrane pads using confocal laser scanning microscopy and high-speed cameras,” *Analytical Chemistry*, vol. 85, no. 7, pp. 3723–3729, 2013.
- [17] Nanocomposix, “Nitrocellulose membrane selection and striping for lateral flow assays,” 2019. [Online]. Available: <https://nanocomposix.com/pages/nitrocellulose-membrane-selection-and-striping-for-lateral-flow-assays>
- [18] “mobile diagnostic lateral flow test strip reader 2019,” 2019. [Online]. Available: <https://mobileassay.com>
- [19] A. Health, “Smartphone lateral flow reader oem,” 2019. [Online]. Available: <https://www.abingdonhealth.com/contract-services/smartphone-lateral-flow-reader-customisation/>
- [20] D. Cooper, D. Cooper, B. Callahan, P. Callahan, and L. Burnett, “Mobile image ratiometry: A new method for instantaneous analysis of rapid test strips,” *Nature Precedings*, 2012.
- [21] M. Abramoff, P. Magelhaes, and S. Ram, “Imagej,” 2019. [Online]. Available: <https://imagescience.org/meijering/publications/download/bio2004.pdf>
- [22] B. A. Cadle, K. C. Rasmus, J. A. Varela, L. S. Leverich, C. E. O’Neill, R. K. Bachtell, and D. C. Cooper, “Cellular phone-based image acquisition and quantitative ratiometric method for detecting cocaine and benzoyllecgonine for biological and forensic applications,” *Substance Abuse: Research and Treatment*, vol. 4, p. SART.S5025, 2010.

- [23] S. Magdassi, M. Grouchko, O. Berezin, and A. Kamyshny, “Triggering the sintering of silver nanoparticles at room temperature,” *ACS Nano*, vol. 4, no. 4, pp. 1943–1948, 2010.
- [24] G. Sergeev and K. Klabunde, “Size effects in nanochemistry,” *Nanochemistry*, pp. 275–297, 2013.
- [25] Z. Wu, S. Yang, and W. Wu, “Shape control of inorganic nanoparticles from solution,” *Nanoscale*, vol. 8, no. 3, pp. 1237–1259, 2016.
- [26] S. Gelperina, K. Kisich, M. D. Iseman, and L. Heifets, “The potential advantages of nanoparticle drug delivery systems in chemotherapy of tuberculosis,” *American Journal of Respiratory and Critical Care Medicine*, vol. 172, no. 12, pp. 1487–1490, 2005.
- [27] A. Akbarzadeh, M. Samiei, and S. Davaran, “Magnetic nanoparticles: preparation, physical properties, and applications in biomedicine,” *Nanoscale Research Letters*, vol. 7, no. 1, p. 144, 2012.
- [28] Z. Wu, S. Yang, and W. Wu, “Shape control of inorganic nanoparticles from solution,” *Nanoscale*, vol. 8, pp. 1237–1259, 2016. [Online]. Available: <http://dx.doi.org/10.1039/C5NR07681A>
- [29] H. Petrova, M. Hu, and G. V. Hartland, “Photothermal properties of gold nanoparticles,” *Zeitschrift für Physikalische Chemie*, vol. 221, no. 3, p. 361–376, 2007.
- [30] S. Eustis and M. A. El-Sayed, “Why gold nanoparticles are more precious than pretty gold: Noble metal surface plasmon resonance and its enhancement of the radiative and nonradiative properties of nanocrystals of different shapes,” *Chem. Soc. Rev.*, vol. 35, no. 3, p. 209–217, 2006.
- [31] J. Perezjuste, I. Pastorizasantos, L. Lizmarzan, and P. Mulvaney, “Gold nanorods: Synthesis, characterization and applications,” *Coordination Chemistry Reviews*, vol. 249, no. 17-18, p. 1870–1901, 2005.
- [32] H. Yuan, A. M. Fales, and T. Vo-Dinh, “Tat peptide-functionalized gold nanostars: Enhanced intracellular delivery and efficient nir photothermal therapy using ultralow irradiance,” *Journal of the American Chemical Society*, vol. 134, no. 28, p. 11358–11361, 2012.
- [33] “Amine gold nanorods (amine-peg3000-sh), 10nm diameter, absorption max 770nm (1ml).” [Online]. Available: <http://www.cytodiagnostics.com/store/pc/Amine-Gold-Nanorods-amine-PEG3000-SH-10nm-diameter-absorption-max-770nm-1ml-p1592.htm>
- [34] “Gold nanostars and immunotherapy vaccinate mice against cancer,” Mar 2018. [Online]. Available: <https://pratt.duke.edu/about/news/symphony>
- [35] H. Kogelnik and T. Li, “Laser beams and resonators,” *Applied Optics*, vol. 5, no. 10, p. 1550, 1966.

- [36] V. Letokhov and V. Minogin, “Laser radiation pressure on free atoms,” *Physics Reports*, vol. 73, no. 1, pp. 1–65, 1981.
- [37] M. Chu, Y. Shao, J. Peng, X. Dai, H. Li, Q. Wu, and D. Shi, “Near-infrared laser light mediated cancer therapy by photothermal effect of fe<sub>3</sub>o<sub>4</sub> magnetic nanoparticles,” *Biomaterials*, vol. 34, no. 16, pp. 4078–4088, 2013.
- [38] H. Liao, C. L. Nehl, and J. H. Hafner, “Biomedical applications of plasmon resonant metal nanoparticles,” *Nanomedicine*, vol. 1, no. 2, pp. 201–208, 2006.
- [39] S. Nie and S. R. Emory, “Probing single molecules and single nanoparticles by surface-enhanced raman scattering,” *Science*, vol. 275, no. 5303, pp. 1102–1106, 1997. [Online]. Available: <http://science.sciencemag.org/content/275/5303/1102>
- [40] E. R. Ziegel and L. Ott, “An introduction to statistical methods and data analysis,” *Technometrics*, vol. 36, no. 3, p. 332, 1994.

## Chapter 8

## Appendix

# List of Figures

3.1	Illustration of a typical configuration of a Lateral Flow Assay composed of a sample pad, membrane, conjugate release pad, backing card, absorbent pad, test line and control line by Dr. Katarzyna M. Koczuła [2] . . . . .	7
3.2	Illustration of the operation of a Lateral FFlow Assay by (Dr.) Katarzyna M. Koczuła [2] . . . . .	8
3.3	An illustration of a Sandwich assay and a Competitive assay with the following reaction in the presence of an antigen [10] . . . . .	9
3.4	Nanoparticles shape classification [28]. . . . .	12
3.5	The shapes of the gold nanoparticles used for the control samples indicating positive results. . . . .	13
4.1	Experimental set up for measurement of increase in temperature of magnetic nanoparticles deposited onto a membrane when exposed to a laser. . . . .	18
4.2	Alignment of mounted magnetic nanoparticles deposited onto a nitrocellulose membrane with a laser. . . . .	19
5.1	Plotted results of change in temperature against time for a series of concentrations of Iron Oxide nanoparticles exposed to a laser on different coloured nitrocellulose membranes. . . . .	21
5.2	Plotted results of change in temperature against time for a series of concentrations of Zinc Ferrite nanoparticles exposed to a laser on different coloured nitrocellulose membranes. . . . .	23
5.3	Temperature differences for nanoparticles on different colored membranes . . . . .	24
5.4	A graph of mean temperature reached by varying sizes of Iron Oxide nanoparticles on different coloured membranes against the concentration of nanoparticles present. Please note the lines of best fit are shown as extrapolated to the left past the data points to illustrate the limit of detection – the concentration at which the mean temperature tends to zero. . . . .	32
5.5	A graph of mean temperature reached by varying sizes of Zinc nanoparticles on different coloured membranes against the concentration of nanoparticles present. Please note the lines of best fit are shown as extrapolated to the left past the data points to illustrate the limit of detection – the concentration at which the mean temperature tends to zero. . . . .	33

5.6	A graph of mean temperature reached by varying sizes of Iron Oxide nanoparticles on different coloured membranes against the concentration of nanoparticles present. Outliers are included in the fit on the left, and removed for the fit on the right. They are plotted in grey on the right. . . . .	34
5.7	A graph of mean temperature reached by varying sizes of Zinc Ferrite nanoparticles on different coloured membranes against the concentration of nanoparticles present. Outliers are included in the fit on the left, and removed for the fit on the right. They are plotted in grey on the right. . . . .	34
5.8	A graph of mean temperature reached by varying sizes of Iron Oxide nanoparticles on different coloured membranes against the concentration of nanoparticles present. Outliers are included in the fit on the left, and removed for the fit on the right. They are plotted in grey on the right. . . . .	35
5.9	A graph of mean temperature reached by varying sizes of Zinc Ferrite nanoparticles on different coloured membranes against the concentration of nanoparticles present. Outliers are included in the fit on the left, and removed for the fit on the right. They are plotted in grey on the right. . . . .	35

# List of Tables

2.1	Table detailing the work done by individual group members on practical and logistical, laboratory, and report based work . . . . .	6
5.1	Statistical significance of a least squares linear fit fitted to experimental data of change in mean temperature of Iron Oxide nanoparticles when exposed to a laser relative to their varying concentration. . . . .	27
5.2	Statistical significance of a least squares linear fit fitted to experimental data of change in mean temperature of Zinc Ferrite nanoparticles when exposed to a laser relative to their varying concentration. . . . .	27
5.3	Statistical significance of a logarithmic fit fitted to experimental data of change in mean temperature of Iron Oxide nanoparticles when exposed to a laser relative to their varying concentration. . . . .	28
5.4	Statistical significance of a logarithmic fit fitted to experimental data of change in mean temperature of Zinc Ferrite nanoparticles when exposed to a laser relative to their varying concentration. . . . .	29
5.5	Statistical significance of a square root fit fitted to experimental data of change in mean temperature of Iron Oxide nanoparticles when exposed to a laser relative to their varying concentration. . . . .	30
5.6	Statistical significance of a square root fit fitted to experimental data of change in mean temperature of Zinc Ferrite nanoparticles when exposed to a laser relative to their varying concentration. . . . .	31

## 8.1 Python Scripts for Data extraction and Analysis

### 8.1.1 Fe<sub>3</sub>O<sub>4</sub>

```
import pandas as pd
import matplotlib.pyplot as plt
import operator
import numpy as np
import scipy.optimize as optimization

from numpy import arange,array,ones
```

```

from scipy import stats

j=1
labels = np.array(["5\u00b0Cg/ml", "10\u00b0Cg/ml", "15\u00b0Cg/ml", "20\u00b0Cg/ml
    ↵ ", "40\u00b0Cg/ml", "50\u00b0Cg/ml", "80\u00b0Cg/ml"])
filename = "Control.csv" # the filename
df = pd.read_csv(filename) # breaking it up into appropriate lists
tmpList = df["Temp"].values.tolist()
yellowcontrol=tmpList[0:6]
bluecontrol=tmpList[6:]

filename = "BlueLarge.csv" # the filename
df = pd.read_csv(filename) # breaking it up into appropriate lists
bluelarge = df["Temperature"].values.tolist()

filename = "YellowLarge.csv" # the filename
df = pd.read_csv(filename) # breaking it up into appropriate lists
yellowlarge = df["Temperature"].values.tolist()

filename = "BlueSmall.csv" # the filename
df = pd.read_csv(filename) # breaking it up into appropriate lists
bluesmall = df["Temperature"].values.tolist()

filename = "YellowSmall.csv" # the filename
df = pd.read_csv(filename) # breaking it up into appropriate lists
yellowsmall = df["Temperature"].values.tolist()

timelist = [30,60,90,120,150,180]
for i in range(int(len(bluelarge)/6)):
    for j in range(6):
        bluelarge[6*i+j]=bluelarge[6*i+j]-bluecontrol[j]
for i in range(int(len(bluesmall)/6)):
    for j in range(6):
        bluesmall[6*i+j]=bluesmall[6*i+j]-bluecontrol[j]

for i in range(int(len(yellowlarge)/6)):
    for j in range(6):
        yellowlarge[6*i+j]=yellowlarge[6*i+j]-yellowcontrol[j]
for i in range(int(len(yellowsmall)/6)):
    for j in range(6):
        yellowsmall[6*i+j]=yellowsmall[6*i+j]-yellowcontrol[j]

```

```

plt.figure(figsize=(7,8))
for i in range(int(len(yellowsmall)/6)):
    plt.scatter(timelist,yellowsmall[6*i:6*(i+1)],label=labels[i])
    slope, intercept, r_value, p_value, std_err = stats.linregress(timelist,
        → yellowsmall[6*i:6*(i+1)])
    point = [30*slope+intercept,180*slope+intercept]
    plt.plot([30,180], point)

plt.xlabel("Time (s)")
plt.ylabel("Differential Temperature ($^\circ$C)")
plt.grid()
plt.xlim(0,250)
plt.ylim(0,35)
plt.legend()

plt.title("Fe$_3$O$_4$ Small Nanoparticles on a Yellow Membrane")

plt.savefig("FeOsmallyyellowTimevTemp.png",dpi=300)

plt.show()

plt.figure(figsize=(7,8))

for i in range(int(len(bluesmall)/6)):
    plt.scatter(timelist,bluesmall[6*i:6*(i+1)],label=labels[i])
    slope, intercept, r_value, p_value, std_err = stats.linregress(timelist,
        → bluesmall[6*i:6*(i+1)])
    point = [30*slope+intercept,180*slope+intercept]
    plt.plot([30,180], point)

plt.grid()

plt.xlabel("Time (s)")
plt.ylabel("Differential Temperature ($^\circ$C)")

plt.xlim(0,250)
plt.ylim(0,15)

plt.legend()

plt.title("Fe$_3$O$_4$ Small Nanoparticles on a Blue Membrane")

```

```

plt.savefig("Fe0smallblueTimevTemp.png",dpi=300)

plt.show()

plt.figure(figsize=(7,8))

for i in range(int(len(yellowlarge)/6)):
    plt.scatter(timelist,yellowlarge[6*i:6*(i+1)],label=labels[i])
    slope, intercept, r_value, p_value, std_err = stats.linregress(timelist,
        ↪ yellowlarge[6*i:6*(i+1)])
    point = [30*slope+intercept,180*slope+intercept]
    plt.plot([30,180], point)

plt.grid()

plt.xlabel("Time (s)")
plt.ylabel("Differential Temperature ($^\circ$C)")
plt.legend()
plt.xlim(0,250)
plt.ylim(0,35)

plt.title("Fe$_3$O$_4$ Large Nanoparticles on a Yellow Membrane")

plt.savefig("Fe0largeyellowTimevTemp.png",dpi=300)

plt.show()

plt.figure(figsize=(7,8))

for i in range(int(len(bluelarge)/6)):
    plt.scatter(timelist,bluelarge[6*i:6*(i+1)],label=labels[i])
    slope, intercept, r_value, p_value, std_err = stats.linregress(timelist,
        ↪ bluelarge[6*i:6*(i+1)])
    point = [30*slope+intercept,180*slope+intercept]
    plt.plot([30,180], point)

plt.grid()

plt.xlabel("Time (s)")
plt.ylabel("Differential Temperature ($^\circ$C)")

```

```

plt.xlim(0,250)
plt.ylim(0,20)

plt.legend()

plt.title("Fe$_3$O$_4$ Large Nanoparticles on a Blue Membrane")

plt.savefig("Fe0largeblueTimevTemp.png",dpi=300)

plt.show()

plt.figure(figsize=(7,8))

for i in range(int(len(bluelarge)/6)):
    plt.scatter(timelist,bluelarge[6*i:6*(i+1)],label=labels[i])
    slope, intercept, r_value, p_value, std_err = stats.linregress(timelist,
        → bluelarge[6*i:6*(i+1)])
    point = [30*slope+intercept,180*slope+intercept]
    plt.plot([30,180], point)

    plt.grid()

    plt.xlabel("Time (s)")
    plt.ylabel("Differential Temperature ($^\circ$C)")

    plt.xlim(0,250)
    plt.ylim(0,20)

    plt.legend()

    plt.title("Fe$_3$O$_4$ Large Nanoparticles on a Blue Membrane")

    plt.savefig("Fe0largeblueTimevTemp.png",dpi=300)

    plt.show()

    plt.figure(figsize=(7,8))

    cap=3
    s=5

```

```

l=0.7

concs=[5,10,15,20,40,50,80]

# small nanoparticles on yellow

smallyellowavgs=[]
smallyellowstd=[]
for i in range(int(len(yellowsmall)/6)):
    avg=np.mean(yellowsmall[6*i:6*(i+1)])
    std=np.std(yellowsmall[6*i:6*(i+1)])
    smallyellowavgs.append(avg)
    smallyellowstd.append(std)
slopesy, interceptsy, r_value, p_value, std_err = stats.linregress(concs,
    ↪ smallyellowavgs)
point = [5*slopesy+interceptsy,80*slopesy+interceptsy]
plt.plot([5,80], point,color="r",linestyle="--")
plt.scatter(concs,smallyellowavgs,label="Small Fe$-3$O$-4$ on Yellow",color="r",
    ↪ s=s)
plt.errorbar(concs,smallyellowavgs,smallyellowstd,linestyle="none",color="r",
    ↪ elinewidth=l,capsize=cap)

# small nanoparticles on blue

smallblueavgs=[]
smallbluestd=[]
for i in range(int(len(bluesmall)/6)):
    avg=np.mean(bluesmall[6*i:6*(i+1)])
    std=np.std(bluesmall[6*i:6*(i+1)])
    smallblueavgs.append(avg)
    smallbluestd.append(std)
slopesb, interceptsb, r_value, p_value, std_err = stats.linregress(concs[0:3],
    ↪ smallblueavgs)
point = [5*slopesb+interceptsb,15*slopesb+interceptsb]
plt.plot([5,15], point,color="b",linestyle="--")
plt.scatter(concs[0:3],smallblueavgs,label="Small Fe$-3$O$-4$ on Blue",color="b",
    ↪ ",s=s")
plt.errorbar(concs[0:3],smallblueavgs,smallbluestd,linestyle="none",color="b",
    ↪ elinewidth=l,capsize=cap)

# large nanoparticles on yellow

```

```

largeyellowavgs=[]
largeyellowstd=[]
for i in range(int(len(yellowlarge)/6)):
    avg=np.mean(yellowlarge[6*i:6*(i+1)])
    std=np.std(yellowlarge[6*i:6*(i+1)])
    largeyellowavgs.append(avg)
    largeyellowstd.append(std)
sloinely, interceptly, r_value, p_value, std_err = stats.linregress(concs,
    ↪ largeyellowavgs)
point = [5*sloinely+interceptly,80*sloinely+interceptly]
plt.plot([5,80], point,color="m",linestyle="--")
plt.scatter(concs,largeyellowavgs,label="Large Fe$-3$O$-4$ on Yellow",color="
    ↪ gold",s=s)
plt.errorbar(concs,largeyellowavgs,largeyellowstd,color="m",linestyle="none",
    ↪ elinewidth=l,capsize=cap)

# large nanoparticles on blue

largeblueavgs=[]
largebluestd=[]
for i in range(int(len(bluelarge)/6)):
    avg=np.mean(bluelarge[6*i:6*(i+1)])
    std = np.std(bluelarge[6*i:6*(i+1)])
    largeblueavgs.append(avg)
    largebluestd.append(std)
slopelb, interceptlb, r_value, p_value, std_err = stats.linregress(concs[0:3],
    ↪ largeblueavgs)
point = [5*slopelb+interceptlb,15*slopelb+interceptlb]
plt.plot([5,15], point,color="c",linestyle="--")
plt.scatter(concs[0:3],largeblueavgs,label="Large Fe$-3$O$-4$ on Blue",color="c
    ↪ ",s=s)
plt.errorbar(concs[0:3],largeblueavgs,largebluestd,color="c",linestyle="none",
    ↪ elinewidth=l,capsize=cap)

plt.grid()
plt.legend()
plt.xlabel("Concentration (\u03bcg/ml)")
plt.ylabel("Mean Temperature ($^\circ$C)")
plt.title("Concentration vs. Mean Temperature for Fe$-3$O$-4$ on different
    ↪ membranes")

```

```

plt.savefig("Fe0ConcentrationvMeanTemp.png",dpi=300)

plt.show()

plt.figure(figsize=(7,8))

labels = ["5\u00b3BCg/ml large","5\u00b3BCg/ml small","10\u00b3BCg/ml large","10\
→ \u00b3BCg/ml small","15\u00b3BCg/ml large","15\u00b3BCg/ml small"]

for i in range(int(len(bluelarge)/6)):
    diff=np.array(bluelarge[6*i:6*(i+1)])-np.array(yellowlarge[6*i:6*(i+1)])
# slope, intercept, r_value, p_value, std_err = stats.linregress(timelist,
#     → bluelarge[6*i:6*(i+1)])
# point = [30*slope+intercept,180*slope+intercept]
# plt.plot([30,180], point)
    plt.plot(timelist,diff,label=labels[2*i])

    diff=np.array(bluesmall[6*i:6*(i+1)])-np.array(yellowsmall[6*i:6*(i+1)])
    plt.plot(timelist,diff,label=labels[2*i+1])
plt.xlabel("Time (s)")
plt.ylabel("T$_B$-T$_Y$ ($^\circ$C)")
plt.title("Temperature difference between Blue and Yellow membranes with
    → Fe$_3$O$_4$")
plt.grid()
plt.legend()

plt.savefig("TempDiffFe0.png",dpi=300)

plt.show()

# large yellow
largeyellow=-interceptly/slovely
# small yellow
smallyellow=-interceptsy/slopesy
# large blue
largeblue=-interceptlb/slopelb
# small blue
smallblue=-interceptsb/slopesb
print(largeyellow,smallyellow,largeblue,smallblue)

```

### 8.1.2 Zn<sub>0.4</sub>Fe<sub>2.6</sub>O<sub>4</sub>

```
import numpy as np
import matplotlib.pyplot as plt
%matplotlib inline
# this command will create graphs in Jupyter notebook # rather than in a separate
    ↪ window
concentration, data_y1_orig = np.loadtxt("ZnFeO_small_yellow.csv", delimiter
    ↪ =';', unpack k=True) # upload data from a file
concentration, data_y2_orig = np.loadtxt("ZnFeO_large_yellow.csv", delimiter
    ↪ =';', unpack k=True) # upload data from a file
concentration, data_y3_orig = np.loadtxt("ZnFeO_small_blue.csv", delimiter=';',
    ↪ unpack= True) # upload data from a file
concentration, data_y4_orig = np.loadtxt("ZnFeO_large_blue.csv", delimiter=';',
    ↪ unpack= True) # upload data from a file
data_x1 = np.array([5, 10, 15, 20, 40, 50, 80]) # create an array of
    ↪ concentration val ues
data_x2 = np.array([5, 15, 20, 40, 50, 80]) # create an array of concentration
    ↪ value s
data_x3 = np.array([10, 15, 20, 40, 50, 80]) # create an array of concentration
    ↪ values data_x4 = np.array([5, 10, 15, 20, 40, 80]) # create an array of
    ↪ concentration values
control1 = np.array([24, 23.3, 23.8, 23.5, 23.6, 23.4]) # create an array of
    ↪ yellow co ntrol temp values
control2 = np.array([24.3, 24.7, 25.3, 25, 24.6, 24.8]) # create an array of
    ↪ blue cont rol temp values
col = np.array(['b', 'r', 'g', 'm']) # array with colour codes for plotting
    ↪ shape = np.array(['o', 's', '^', '*'])
legends = np.array(["$Zn_{0.4}Fe_{2.6}O_4$ small, yellow membrane",
"$Zn_{0.4}Fe_{2.6}O_4$ large, yellow membrane", "$Zn_{0.4}Fe_{2.6}O_4$ small,
    ↪ blue membrane", "$Zn_{0.4}Fe_{2.6}O_4$ large, blue membrane"])
# subtract the control values from the actual temperature values
j=0
data_y1 = np.zeros(len(data_y1_orig))
# every 6 values in data_x array start subtracting from the first value # of the
    ↪ control array again
for i in range(0, len(data_y1_orig)):
    data_y1[i] = data_y1_orig[i] - control1[j] j += 1
if(j == 6):
    j=0
j=0
```

```

data_y2 = np.zeros(len(data_y2_orig))
# every 6 values in data_x array start subtracting from the first value # of the
    ↪ control array again
for i in range(0, len(data_y2_orig)):
    data_y2[i] = data_y2_orig[i] - control1[j] j += 1
if(j == 6):
    j=0
j=0
data_y3 = np.zeros(len(data_y3_orig))
# every 6 values in data_x array start subtracting from the first value # of the
    ↪ control array again
for i in range(0, len(data_y3_orig)):
    data_y3[i] = data_y3_orig[i] - control2[j] j += 1
if(j == 6):
    j=0
j=0
data_y4 = np.zeros(len(data_y4_orig))
# every 6 values in data_x array start subtracting from the first value # of the
    ↪ control array again
for i in range(0, len(data_y4_orig)):
    data_y4[i] = data_y4_orig[i] - control2[j] j += 1
if(j == 6):
    j=0
# find the average temperature and error for each concentration
data_y1_ave = np.zeros(7)
data_y2_ave = data_y3_ave = data_y4_ave = np.zeros(6)
data_y1_ave_err = np.zeros(7)
data_y2_ave_err = data_y3_ave_err = data_y4_ave_err = np.zeros(6)
for i in range(0, 7):
    data_y1_ave[i] = np.mean(data_y1[(i*6):((i+1)*6)]) data_y1_ave_err[i] = np.std(
        ↪ data_y1[(i*6):((i+1)*6)])
for i in range(0, 6):
    data_y2_ave[i] = np.mean(data_y2[(i*6):((i+1)*6)]) data_y2_ave_err[i] = np.std(
        ↪ data_y2[(i*6):((i+1)*6)])
for i in range(0, 6):
    data_y3_ave[i] = np.mean(data_y3[(i*6):((i+1)*6)]) data_y3_ave_err[i] = np.std(
        ↪ data_y3[(i*6):((i+1)*6)])
for i in range(0, 6):
    data_y4_ave[i] = np.mean(data_y4[(i*6):((i+1)*6)]) data_y4_ave_err[i] = np.std(
        ↪ data_y4[(i*6):((i+1)*6)])
# define a function that will be plotting least square fit straight lines

```

```

def least_square_fit(data_x, data_y, data_y_err, j):
    mean_x = np.mean(data_x) # calculate mean value of x coordinates
    mean_y = np.
        ↪ mean(data_y) # calculate mean value of y coordinates
    m = np.sum((data_y - mean_y)*data_x) / np.sum((data_x - mean_x)*data_x) c =
        ↪ mean_y - m*mean_x
    n = len(data_x) # calculate the number of pairs of coordinates
    D_calc = np.sum((
        ↪ data_x - mean_x)**2)
    sum_d2 = np.sum((data_y - m*data_x - c)**2)
    dm = np.sqrt(sum_d2 / (D_calc*(n-2))) # calculate uncertainty in m
    dc = np.sqrt(((1/n) + (mean_x**2/D_calc)) * (sum_d2 / (n-2)))
    anity in c
    # create two arrays
    fit_x = np.linspace(np.min(data_x), np.max(data_x), 2)
    fit_y = m * fit_x + c
    # plot the line
    plt.plot(fit_x, fit_y, '--', color=col[j])
    # plot the data points
# calculate uncert
    plt.errorbar(data_x, data_y, fmt=shape[j], yerr=data_y_err, color=col[j],
        ↪ label=leg
ends[j])
plt.figure(figsize=(7,8))
least_square_fit(data_x1, data_y1_ave, data_y1_ave_err, 0)
least_square_fit(data_x2, data_y2_ave, data_y2_ave_err, 1)
least_square_fit(data_x3, data_y3_ave, data_y3_ave_err, 2)
least_square_fit(data_x4, data_y4_ave, data_y4_ave_err, 3)
# plt.errorbar(data_x4, data_y4_ave, fmt='o', yerr=data_y4_ave_err, color=col[3],
    ↪ label= legends[3])
# set the graph parametres
plt.grid(True)
plt.title("Concentration vs. Mean Temperature for $Zn_{0.4}Fe_{2.6}O_4$ on
    ↪ different me mbranes")
plt.legend(loc="lower right")
plt.xlim(0, 100)
plt.ylabel("Mean Temperature, \u00b0C")
plt.xlabel("Concentration, \u03bcg/ml")
plt.savefig("ZnFeO_conc_vs_temp.png", dpi = 300)
data_y4 = np.append(data_y4[:6], data_y4[12:])
data_y2 = np.append(data_y2[:24], data_y2[30:])
time = np.array([30, 60, 90, 120, 150, 180])
new_data_y1 = data_y3[:] - data_y1[6:]

```

```

col = np.array(['b', 'r', 'g', 'm', 'c', 'k']) # array with colour codes for
    ↪ plotting labels = np.array(["10\u03BCg/ml", "15\u03BCg/ml",
"20\u03BCg/ml", "40\u03BCg/ml", "50\u03BCg/ml", "80\u03BCg/ml"])
# define a function that will be plotting least square fit straight lines
def least_square_fit1(data_x, data_y, j):
mean_x = np.mean(data_x) # calculate mean value of x coordinates mean_y = np.
    ↪ mean(data_y) # calculate mean value of y coordinates
m = np.sum((data_y - mean_y)*data_x) / np.sum((data_x - mean_x)*data_x) c =
    ↪ mean_y - m*mean_x
n = len(data_x) # calculate the number of pairs of coordinates D_calc = np.sum((
    ↪ data_x - mean_x)**2)
sum_d2 = np.sum((data_y - m*data_x - c)**2)
dm = np.sqrt(sum_d2 / (D_calc*(n-2))) # calculate uncertainty in m
dc = np.sqrt(((1/n) + (mean_x**2/D_calc)) * (sum_d2 / (n-2)))
# create two arrays
fit_x = np.linspace(np.min(data_x), np.max(data_x), 2)
fit_y = m * fit_x + c
# plot the line
plt.plot(fit_x, fit_y, '-.', color=col[j])
# plot the data points
plt.plot(data_x, plot_y, 'o', color=col[j], label = labels[j])
# calculate uncertainty in c
plt.figure(figsize=(7,8))
# plot data points 7 times
start = 0
end = 6
for i in range(0, 6):
plot_y = new_data_y1[start:end] least_square_fit1(time, plot_y, i) start = end
end += 6
# set the graph parametres
plt.grid(True)
plt.title("Temperature Difference Between Blue and Yellow membranes with $Zn_
    ↪ {0.4}Fe_ {2.6}O_4$")
plt.legend(loc="lower right")
plt.xlim(0, 250)
plt.ylabel("$T_B - T_Y$, (\u00b0C)")
plt.xlabel("Time (s)")
plt.savefig("Temp_diff_small.png", dpi = 300)

import numpy as np
import matplotlib.pyplot as plt

```

```

%matplotlib inline
# this command will create graphs in Jupyter notebook # rather than in a separate
    ↪ window
concentration, data_y = np.loadtxt("ZnFeO_large_yellow.csv", delimiter=';',
    ↪ unpack=True ) # upload data from a file
control = np.array([24.3, 24.7, 25.3, 25, 24.6, 24.8]) # create an array of blue
    ↪ control temp values
data_x = np.arange(30, 181, 30) # create an array of time values
#data_x = np.tile(data_x, 7)
col = np.array(['b', 'r', 'g', 'm', 'c', 'k']) # array with colour codes for
    ↪ plotting labels = np.array(["5\u00d71023BCg/ml", "10\u00d71023BCg/ml", "15\u00d71023BCg/ml
    ↪ ",
"20\u00d71023BCg/ml", "40\u00d71023BCg/ml", "80\u00d71023BCg/ml"])
# subtract the control values from the actual temperature values
j=0
data_y_corr = np.zeros(len(data_y))
# every 6 values in data_x array start subtracting from the first value # of the
    ↪ control array again
for i in range(0, len(data_y)):
    data_y_corr[i] = data_y[i] - control[j]
    j += 1
if(j == 6):
    j=0
# define a function that will be plotting least square fit straight lines
def least_square_fit(data_x, data_y, j):
    mean_x = np.mean(data_x) # calculate mean value of x coordinates
    mean_y = np.mean(data_y) # calculate mean value of y coordinates
    m = np.sum((data_y - mean_y)*data_x) / np.sum((data_x - mean_x)*data_x)
    c = mean_y - m*mean_x
    n = len(data_x) # calculate the number of pairs of coordinates
    D_calc = np.sum((data_x - mean_x)**2)
    sum_d2 = np.sum((data_y - m*data_x - c)**2)
    dm = np.sqrt(sum_d2 / (D_calc*(n-2))) # calculate uncertainty in m
    dc = np.sqrt(((1/n) + (mean_x**2/D_calc)) * (sum_d2 / (n-2)))
    # calculate uncertainty in c
    # create two arrays
    fit_x = np.linspace(np.min(data_x), np.max(data_x), 2)
    fit_y = m * fit_x + c
    # plot the line
    plt.plot(fit_x, fit_y, '-.', color=col[j])
    # plot the data points
# calculate uncert

```

```

plt.plot(data_x, plot_y, 'o', color=col[j-1], label = labels[j-1])
plt.figure(figsize=(7,8))
# plot data points 7 times
start = 0 end = 6 j=1
for i in range(0, 6):
plot_y = data_y_corr[start:end] least_square_fit(data_x, plot_y, j) start = end
end += 6
j += 1
# set the graph parameters
plt.grid(True)
plt.title("$Zn_{0.4}Fe_{2.6}O_4$ Large Nanoparticles on a Blue Membrane") plt.
    ↪ legend(loc="upper right")
plt.xlim(0, 250)
plt.ylabel("Differential Temperature, \u00b0C")
plt.xlabel("Time, s")
plt.savefig("ZnFeO_large_blue.png", dpi = 300)

```

## 8.2 Finances

### 8.2.1 Total Covered Costs

GE Whatman X10 FF170HP Membranes 200µm thickness - £91.78

Poster- £30-40

Project Binding- £60-80

### 8.2.2 Membranes



Your order number F60-2783446 of 11/02/19

#### ORDER CONFIRMATION N° 1152753170

11/02/2019

Fisher Scientific UK Ltd  
Bishop Meadow Road  
Loughborough  
Leicestershire  
LE11 5RG UK  
UNITED KINGDOM

Website [www.fisher.co.uk](http://www.fisher.co.uk)

Delivery address  
UNIVERSITY COLLEGE LONDON  
ROOM E15  
PHYSICS & ASTRONOMY  
GOWER PLACE  
LONDON  
WC1E 6BN  
GREAT BRITAIN  
Skipper, Prof Neal

Confirmation address ID number 3165924  
UNIVERSITY COLLEGE LONDON  
ROOM E15  
PHYSICS & ASTRONOMY  
GOWER PLACE  
LONDON  
WC1E 6BN  
UNITED KINGDOM

Debtor address  
UNIVERSITY COLLEGE LONDON  
ACCOUNTS PAYABLE  
UCL FINANCE & BUSINESS AFFAIRS  
GOWER STREET  
LONDON  
WC1E 6BT

#### For enquiries on

Customer Services

Phone 01509555500

Fax 01509555111

Email [fisheruk.orders@thermofisher.com](mailto:fisheruk.orders@thermofisher.com)

Item No.	Item Description	Qty ordered	UOM	Unit Price	Total net price	Dispatch date (estimated)
External DI Order Del.Instr	Y Skipper, Prof Neal Physic					
15552656	X10 FF170HP Membranes Din A4. 200µm thickness, wit h a material backing of polyester Customer line n 1 Fisher Brand GE Healthcare Whatman Each (EA) = 1 x 10.00 PCS	1	EA	91.78	91.78	26/02/2019

Currency GBP

Terms of delivery	CFR	
Manner of transport	Road	Total amount without VAT
Payment terms	30 days net	91.78

Page : 1 / 1

Fisher Scientific UK Limited  
Bishop Meadow Road  
Loughborough, Leics  
LE11 5RG, United Kingdom  
Unless otherwise specifically agreed in writing, all sales are subject to Fisher Scientific's standard terms and conditions.  
[www.eu.fishersci.com/go/terms](http://www.eu.fishersci.com/go/terms) Registered Office: Bishop Meadow Road, Loughborough, Leicestershire, LE11 5RG, United Kingdom. Registered in England No. 2883961.

### 8.2.3 Thermochromic Sheets



Special Effects & Coatings

[sales@sfxc.co.uk](mailto:sales@sfxc.co.uk)

0800 999 3123

#### Billing Address

Accounts Payable University  
college london  
University college london  
Gower street,  
UCL finance and business  
affairs  
London  
United Kingdom  
WC1E 6BT

#### Shipping Address

Thithawat Trakoolwilaiwan  
Royal Institution of Great Britain  
21 Albemarle street,  
London  
United Kingdom  
W1S 4BS

### Invoice

**Return Address:**  
Unit 6, Newhaven Enterprise Centre, Denton Island, Newhaven, East Sussex,  
BN9 9BA



DC-1551081810-247

**Order(s):** 910814609492

**Payment Type:**

**Special Instructions:** No

**Shipping Requested:** Express (1 to 2 working days)

**Order Date:** 22 Feb 2019 15:41 PM

**Sales Channel:** SFXC

**Special Files:** No

Qty	SKU	Location	Image	Product	Unit Price
1 ✓	8K-223G-WHWC	Laboratory One		Liquid Crystal Thermochromic Colour Changing Sheet - 300mm by 450mm / 40°C to 45°C	34.00
1 ✓	1A-0749-LEL9	Laboratory One		Liquid Crystal Thermochromic Colour Changing Sheet - 300mm by 450mm / 30°C to 35°C	34.00
1 ✓	3D-VFRP-045P	Laboratory One		Liquid Crystal Thermochromic Colour Changing Sheet - 300mm by 450mm / 25°C to 30°C	34.00
1 ✓	NC-12TR-LWDV	Laboratory One		Liquid Crystal Thermochromic Colour Changing Sheet - 300mm by 450mm / 35°C to 40°C	34.00

<b>Shipping:</b>	12.00
<b>VAT:</b>	24.67
<b>Total (GBP):</b>	148.00

**Total Items:** 4

Company Registration No: 07003596 VAT No: 122703551

Powered by Despatch Cloud (<http://despatch.cloud>)

## 8.3 Risk Assessment

<b>HEALTHCARE BIOMAGNETICS LABORATORIES</b> 21 ALBEMARLE STREET, LONDON, W1S 4BS		
<b>RISK ASSESSMENT FORM FOR EXPERIMENTAL PROCEDURES 2013-14</b> <i>(REFER TO THE GUIDELINES PAGE 2 IF NECESSARY)</i>		
<b>Risk Rating (H= High, M= Medium, L= Low):</b> Low	<b>Dates of the experiments/procedures:</b> January 2019-March 2019	
<b>Title of Experiment/Procedure:</b> Investigation on the thermal contrast of thermochromic sheet against photothermal nanoapticles	<b>Personnel involved (incl. status):</b> MSc. Thithawat Trakoolwilaiwan PhD Francesco Rossi Grace Hymas Ivan Popov Sean MacBride Anja Rellstab Amitpal Basi Jennifer Lin Abby Goh Wehao Wu	
<b>Equipment to be used:</b> Sonicator	<b>Lab(s) in which work will take place:</b>	
<b>Substances (including quantities):</b> Iron Oxide Nanoparticles Zinc Ferrite ( $Zn_{0.4}Fe_{2.6}O_4$ ) Nanoparticles Gold Nanoparticles  All particles are suspended in water.	<b>Hazards identified (chemical, biological, electrical, manual handling etc):</b>  Zinc ferrite NPs and iron oxide NPs are not hazardous substances or mixtures, according to Regulation (EC) No.1272/2008. However, exposing to, consuming, or inhaling such nanoparticles should be avoided.  For gold nanoparticles, $AgNO_3$ toxic to aqueous $NaBH_4$ , toxic when ingested and toxic to skin	
<b>Information sources (i.e. MSDS etc):</b> MSDS from sigma-Aldrich		
<b>Control measures to be adopted:</b> Gloves, safety glasses and lab coat are worn for all lab works. Washing hands with soap properly after involving with the substances.		
<b>Emergency Procedures (if any of the substances or procedures identified are likely to pose a special hazard in an emergency, then identify below the action to be taken):</b>  <b>If inhaled</b> move person into fresh air. <b>Skin contact</b> Wash off with soap and plenty of water. <b>Eye contact</b> Flush eyes with water as a precaution. <b>Swallowed</b> Rinse mouth with water.		
Is this procedure authorised to be carried out outside normal working hours? Yes <input type="checkbox"/> No <input checked="" type="checkbox"/>		
Is this procedure authorised to be left unattended? No <input type="checkbox"/> Yes, but only during standard working hours <input type="checkbox"/> Yes, at any time <input checked="" type="checkbox"/>		
<b>Disposal procedures during and at end of experiment:</b> Non-halogenated solvent waste Halogenated solvent waste		

<b>Assessor:</b> I have been given a safety induction <input type="checkbox"/>	Signed:	DATE
<b>Project Supervisor(s):</b>	Signed:	DATE
<b>Lab manager/Safety Officer:</b>	Signed:	DATE

Anyone other than the assessor involved in a project to which this assessment relates should sign the statement below (continue on a separate page if necessary):

I have read this document and understand it and have approval to use the equipment listed.

Name (print) ... <u>IVAN POPOV</u>	Signed .....	Date <u>23/01/19</u>
Name (print) ... <u>GRACE HYMAS</u>	Signed .....	Date <u>23/01/19</u>
Name (print) ... <u>Amritpal Basit</u>	Signed .....	Date <u>23/01/19</u>
Name (print) ... <u>Wenhsia Wu</u>	Signed .....	Date <u>23/01/19</u>
Name (print) ... <u>Angela Rebabab</u>	Signed .....	Date <u>23/01/19</u>
Name (print) ... <u>Aisling Bohm</u>	Signed .....	Date <u>23/01/19</u>
Name (print) ... <u>Jennifer Wu</u>	Signed .....	Date <u>23/01/19</u>
Name (print) ... <u>Sean MacBride</u>	Signed .....	Date <u>23/01/19</u>

**Personal Protective Equipment:** Please list any personal protective equipment required for the handling of specific chemicals. Examples may include gloves, aprons, lab coats, including any required protective clothing (e.g. lab coat or smock) and any other relevant items.

**Emergency Procedures:** A plan must be in place to deal with accidental exposure to hazardous materials, leakage, fire etc.

**Starting Experiments Unattended:** for low-risk procedures only. It may be necessary to leave the room during such an experiment.

**Shutting Down:** All procedures MUST comply with shutdown procedures to cause further hazards or damage to others.

**Other:** Any new equipment must be checked by the supervisor before being used. If any equipment, apparatus and substances used pose a hazard to health, a risk assessment needs to be carried out and the person in charge must take action.

#### NOTES ON PERSONNEL

**PROJECT SUPERVISOR:** I declare that I am fully aware of the potential risks associated with my work. Should I gain any new knowledge about the potential risks, I will change my working practices with immediate effect.

**PROJECT SUPERVISOR:** The project supervisor is responsible for the safety of all staff members. Quentin Pandurust or Thanh Nguyen are available to answer any questions about the work. They should be approached at the earliest opportunity if any changes are made to the work. They suggest amendments or additions to the procedure.

**LAB MANAGER/SAFETY OFFICER:** I am responsible for the safety of my department. I will advise my supervisor if any new risks are identified.

**Guidelines for filling in the Risk Assessment form:**

**Risk rating:** an overall assessment of the risk involved (to be filled when the overall assessment has been completed).

- **HIGH** – serious risk of injury to personnel. Experiment not to be carried out by untrained personnel. It may be necessary to have extra personnel standing by in case of accidents.
- **MEDIUM** – some risk to personnel, which can be minimised by having proper precautions in place (these precautions MUST be outlined on the form, and MUST be in place each time the experiment is performed)
- **LOW** – little or no risk to personnel. (note: even if the risk is low, the assessment must still be carried out)

**Lab(s) used:** a list of the rooms in which the experimental work will take place (e.g. E10 – workshop and microscopy; E18 – chemistry 1)

**Substances involved:** a complete list of the chemical and biological materials used in the experiment.

**Hazards identified:** The following list should be considered in the assessment: Chemical (Toxic by inhalation? Toxic by contact? Harmful? Irritant? Volatile? Lachrymator?), Biological, Dust, Electrical, Explosive, Compressed Gas, Fire, Laser/UV/Radiation, Manual Handling. Remember that the SCALE of the experiment will also affect the level of risk involved (something safe on a microlitre scale may be hazardous on a multi-litre scale)

**Information Source:** the MSDS supplied with most materials will outline any associated hazards (and should be attached to the RA form)

**Control measures:** Example, a fumehood (with sufficient airflow!) for the handling of volatile chemicals. Temperature controls for exothermic processes. Include any required protective clothing (gloves/lab coats/safety glasses) in this section.

**Emergency procedures:** a plan must be in place to deal with accidental exposure to hazardous materials, spillage, fire etc.

**Running Experiments Unattended:** for low-risk procedures only. It may be useful to leave some contact details near the experimental set-up

**Disposal procedure:** MUST comply with legislation, and must not cause further hazards or nuisance to others.

**Safety induction:** any new personnel must be given a safety induction for all equipment, laboratories and substances they are handling. In addition, a fire safety induction needs to be carried out, and the personnel shown all fire exits.

---

**NOTES ON PERSONNEL:**

**ASSESSOR:** Usually the researcher or student carrying out the experimental activity. Should have sufficient knowledge about the hazards involved, or ask advice from someone with greater expertise.

**PROJECT SUPERVISOR:** The project supervisors should be the Principal Investigator (e.g. Quentin Pankhurst or Thanh Nguyen) and any lab personnel supervising/overseeing the work. They should only sign the form if confident that the risks have been assessed correctly. May suggest amendments or additions to the risk assessment.

**LAB MANAGER/SAFETY OFFICER:** Either Steve Nesbitt or your departmental safety officer may sign the form, once they are satisfied with the assessment.

## 8.4 Lab Book

31/01/19 - Grace Hymas, Sean MacBride, Ivan Popov

**Aims:**

- To find the limit of detection of our Lateral Flow Assay (LFA) design
- To use LFA's and accessible technologies (e.g. smartphones) to qualitatively identify the concentration of the nanoparticles in the solution
- Quantitatively measure the correlation between temperature of the excited nanoparticles and the concentration of nanoparticles in the solution

**Objectives:**

- Use a control marker and background subtraction to standardise the colour intensity results
  - Create/use existing software to analyse images of the thermochromic sheets under the test line
- Find the real output the laser & general environment of laser (are we able to use same setup or will other team be using it in intermediary)
- To deposit the nanoparticles on a nitrocellulose membrane and activate it with an appropriate powered laser in order to test the concentration of nanoparticles in the solution, using the test line of antibodies
- Test different concentrations of nanoparticles in the solution and correspond them to intensity of colour of the test line and the heat produced by the test line measured by IR camera and thermochromic sheets

**WORK NOTES:**

Picked up chemicals from Thithawat at the Royal Institute. Chemicals are labelled:

- Iron oxide ( $\text{Fe}_3\text{O}_4$ ) small 10mg/mL
- Iron oxide ( $\text{Fe}_3\text{O}_4$ ) big 15mg/mL
- Zinc ferrite ( $\text{Zn}_0.4\text{Fe}_2.6\text{O}_4$ ) small 7.3mg/mL
- Zinc ferrite ( $\text{Zn}_0.4\text{Fe}_2.6\text{O}_4$ ) big 7.5mg/mL

Need to do risk assessment on laser and push Thithawat for other risk assessment.

Need to write theory (written FORMALLY as you would in a proper assessed lab book, all theory must be in relation to the experiment, not just random) and find out more about experimental method.

- Nanoparticles
- LFAs (general theories and types)
- Nitrocellulose membranes
- Laser theory
- Thermochromic sheets

Literature review needs to be finished FORMALLY.

Write up from people doing literature review if they found any methods or technologies or side projects we can do in our experiment from the literature review (there should definitely be some if the literature review was done on the right things!).

More research on other lasers (maybe HEP).

Need to find out when we can actually use the lab with the laser (in UCL).

Presentation at the end of every week by any teams to let everyone know what each other have found in the week so everyone is kept up to date.

Sean has chemicals.

All above points relayed to team 31/01/2019.

### **06/02/2019 - Grace Hymas**

#### **Notes to relay in meeting:**

- Perhaps we could do some study on uses of magnetic nanoparticles for treating diseases etc?  
And where they have been used before for testing.
- Maybe look into ferrite nanoparticles with silica shell? These can be fluorescent (easier to use and see on our test strip) and possess a lot of improved physical properties.
- Could we detect the magnetic field of the nanoparticles instead of using heat?
- Can people add anything to theory they have found in lit review that may be useful here?

#### **Theory NEED TO DO REFERENCE FOR ALL OF THIS**

- Nanoparticles
- LFAs (general theories and types)
- Nitrocellulose membranes
- Laser theory
- Thermochromic sheets

#### **(Magnetic) Nanoparticles**

A nanoparticle simply is a microscopic particle with at least one dimension less than 100 nm. They are useful due to the fact that they bridge the gap between bulk materials and molecular structures due to their intermediate size. They are composed of one metal element and one chemical element making them often susceptible to magnetic fields.

Iron oxide becomes superparamagnetic when smaller than a few hundred nanometres.

Nanoparticles have a very high surface area to volume ratio, providing a tremendous driving force for diffusion, especially at elevated temperature (i.e. with a laser). This also causes the melting temperature of the nanoparticles to be significantly lower, which could contribute to error.

Sintering (the welding together of small particles of metal by applying heat below the melting point) can take place at lower temperatures, over shorter time scales than for larger particles. This theoretically does not affect the density of the final product, though flow difficulties and the tendency of nanoparticles to agglomerate complicates matters. This could be a source of uncertainty!

Iron oxide:

- 1 - 100 nm diameter
- superparamagnetic

Zinc ferrite:

- Around 40nm
- Not a lot of info on these!

Gold:

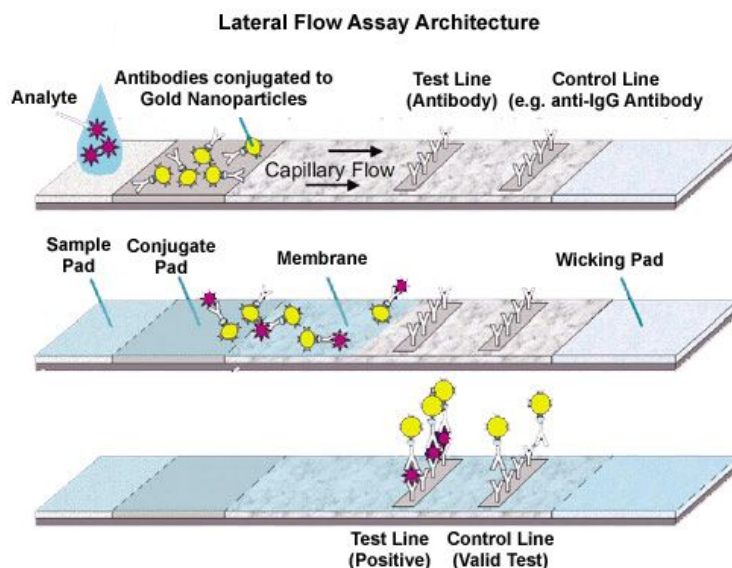
- 5-100nm diameter typically (although can be up to 400nm).
- Surface plasmon resonance causes light absorbing properties and strong colour in solution.

### Lateral Flow Assays

A lateral flow test contains several important components as shown in the diagram below:

- Sample pad: an absorbent pad onto which the test sample is applied.
- Conjugate or reagent pad: this contains antibodies specific to the target analyte conjugated to coloured particles (usually colloidal gold nanoparticles, or latex microspheres).
- Reaction membrane – typically a nitrocellulose or cellulose acetate membrane onto which anti-target analyte antibodies are immobilized in a line that crosses the membrane to act as a capture zone or test line (a control zone will also be present, containing antibodies specific for the conjugate antibodies).
- Wick or waste reservoir – a further absorbent pad designed to draw the sample across the reaction membrane by capillary action and collect it.

The components of the strip are fixed to an inert backing material.



STEPS: The sample pad acts as a sponge and holds an excess of sample fluid. Once soaked, the fluid migrates to the conjugate pad in which the manufacturer has stored the conjugate, a dried format of bio-active particles in a salt-sugar matrix that contains everything to guarantee an optimized chemical reaction between the target molecule (e.g., an antigen) and its chemical partner (e.g., antibody) that has been immobilized on the particle's surface. While the sample fluid dissolves the salt-sugar matrix, it also dissolves the particles, and in one combined transport action, the sample and conjugate mix while flowing through the porous structure. In this way, the analyte binds to the particles while migrating further through the third capillary bed. This material has one or more areas (often called stripes) where a third molecule has been immobilized by the manufacturer. By the time the sample-conjugate mix reaches these strips, analyte has been bound on the particle and the third "capture" molecule binds the complex. After a while, when more and more fluid has passed the stripes, particles accumulate and the stripe-area changes color. Typically, there are at least two stripes: one (the control) that captures any particle and thereby shows that reaction conditions and technology worked fine and one that contains a specific capture molecule and only captures those particles onto which an analyte molecule has been immobilized. After passing these reaction zones, the fluid enters the final porous material, the wick, that simply acts as a waste container.

### Laser Theory

### Thermochromic Sheets

**08/02/2019 - Grace Hymas, Ivan Popov**

### Experimental Method

We must:

- Create a laser exposure time curve to work out which exposure time is best for which concentration (see Francesco's methods)
- MUST keep distance from laser to LFA constant
- Vary concentration of nanoparticles from low to high (recommended 25 and 200 micrograms per mL).
- Vary the size of the membrane, although we should begin with around 5cm long to 2cm wide.
- Vary the laser exposure time, although long times should be started with (10 minutes perhaps depending greatly on the strength of the laser we manage to find).
- Take LFA without the solution applied to it (Empty LFA), and expose the test line to the laser. Measure the temperature. Repeat for other LFA's without the solution, compare the temperatures. Make sure to label each LFA. Compare the temperatures of the excited test line before and after applying the solution. Compare the temperatures of excited test lines of different LFA's with the same concentration of nanoparticles in the solution applied. Plot a graph of excitation temperatures before and after applying the solution with the same concentration of nanoparticles.

- How do we apply the thermochromic sheet to the assay? I think under the assay or as strips on the assay of different thermochromic sheets. We can't place thermochromic sheets/ink as strips on the assay. This way it will be not in contact with the test line that we will heat up with the laser, but next to it. So the only way to place thermochromic materials is under the assay [1]. The best way is to use thermochromic ink.
- Analyse the colour intensity of the sheets with a software to determine which sheet is correct for the concentration and therefore what concentration is present (and link to intensity of disease). The best way to go about it is to use IR camera to determine the excitation temperatures for different concentrations of nanoparticles in the solution. Then find thermochromic materials with the activation temperature regions corresponding to the excitation temperature for the particular concentration (e.g. for concentration 200 micrograms per mL excitation temperature is 35 degrees Celsius, so we need thermochromic material with activation region 30-40 degrees Celsius). We can produce a range of LFA's each of which will be sensitive only to a specific concentration of nanoparticles in the solution. So when being irradiated with the same laser for the same time, the only thermochromic material to change colour will be the one on LFA for corresponding concentration. So the concentration can be determined quantitatively. Possible disadvantages of such method: the excitation temperatures for different concentrations may only vary by few degrees, and the thermochromic materials will only have activation regions as narrow as 10 degrees.
- Repeat to gain as much data as possible!
- Since we don't have a sample pad, we are going to use a pipet to apply the solution to a membrane. We need to ensure that we control the amount of fluid applied to the membrane.

All parameters will depend on the strength of the laser, we will need higher everything if the laser power is lower.

[1] - Adam C. Siegel et al., "Thin, lightweight, foldable thermochromic displays on paper."

Magnetic nanoparticles sizes:

small iron oxide = 10.4 +- 2.6 nm  
 small zinc ferrite = 11.0 +- 1.8 nm  
 large iron oxide = 13.12 +- 2.1 nm  
 large zinc ferrite = 15.13 +- 2.25 nm

#### **08/02/2019 - Jennifer Lin**

- RE to the thermochromic sheet experimental method: we could try both methods, first one with the one thermochromic sheet (and use this approach for sheets of different activation temperatures). In the second method we place different thermochromic sheets together so that we could determine the temperature of the strip after the laser activation. In both cases, the purpose of using the thermochromic sheets is that the LFA will display a colour which could be analysed.
- In addition to nanoparticles, will we have any chance of integrating the use of magnetic nanoparticles with the actual solutions which contain antibodies? (So that we could prove that magnetic nanoparticles in fact bind to antigens in the solutions when we test our LFAs)

#### **19/02/2019 - Grace Hymas**

PARTICLE SIZES:

small iron oxide = 10.4 +- 2.6 nm  
small zinc ferrite = 11.0 +- 1.8 nm  
large iron oxide = 13.12 +- 2.1 nm  
large zinc ferrite = 15.13 +- 2.25 nm

**22/02/2019 - Ivan Popov and Grace Hymas - IN LAB RI**

Todays Aims:

- Produce solutions with various concentrations from the available nanoparticles.
- Deposit solutions onto membranes.

NOTE: Membranes arrived today at UCL - we need to pick up.

Calculations

Our solution of Fe<sub>3</sub>O<sub>4</sub> small contains 10µg/ml Fe<sub>3</sub>O<sub>4</sub>. Therefore to dilute our required concentration of 20µg/ml we must calculate:

$$\frac{20}{10000} \times 1000 = 2\mu l$$

So if we take 2µl of solution we will get 20µg of the nanoparticles. General formula:

$$\frac{\text{required concentration}}{\text{given concentration}} \times 1000$$

Then we can add the remaining solution (water) to make the total amount 1000µl. In the case of our example, we would use 998µl of water.

Required Concentration (µg/ml)	Required Amount of Nanoparticle in µg			
	Iron Oxide Fe <sub>3</sub> O <sub>4</sub>		Zinc Ferrite Zn0.4Fe2.6O4	
	Small 10mg/ml	Large 15mg/ml	Small 7.3mg/ml	Large 7.5mg/ml
20	A 2.00	E 1.33	I 2.74	M 2.67
40	B 4.00	F 2.67	J 5.48	N 5.33
50	C 5.00	G 3.33	K 6.85	O 6.67
80	D 8.00	H 5.33	L 10.96	P 10.67

Figure 1: Required amounts of nanoparticles required to give a given concentration. Note that all nanoparticle solutions will be 1000µl so the given amounts will be topped up with this amount of water. Letters are used here for ease of reference at all points later in the script.

Error on pipette used is 0.05µl (as this is the degree to which it measures). Each value below had been rounded to the nearest 0.05µl. Therefore final nanoparticle solutions will be:

A: 2.00µg with 998.00µg water

B: 4.00µg with 996.00µg water

C: 5.00 $\mu$ g with 995.00 $\mu$ g water  
D: 8.00 $\mu$ g with 992.00 $\mu$ g water  
E: 1.35 $\mu$ g with 998.65 $\mu$ g water  
F: 2.65 $\mu$ g with 997.35 $\mu$ g water  
G: 3.35 $\mu$ g with 996.65 $\mu$ g water  
H: 5.35 $\mu$ g with 994.65 $\mu$ g water  
I: 2.75 $\mu$ g with 997.25 $\mu$ g water  
J: 5.50 $\mu$ g with 994.50 $\mu$ g water  
K: 6.85 $\mu$ g with 993.15 $\mu$ g water  
L: 10.95 $\mu$ g with 989.05 $\mu$ g water  
M: 2.65 $\mu$ g with 997.35 $\mu$ g water  
N: 5.35 $\mu$ g with 994.65 $\mu$ g water  
O: 6.65 $\mu$ g with 993.35 $\mu$ g water  
P: 10.65 $\mu$ g with 989.35 $\mu$ g water

#### Method for Diluting Nanoparticles

1. Put required amount of water into small beaker with high accuracy pipette.
2. Take required amount of nanoparticles and put into water.
  - NOTE: There are nanoparticles left in the pipette, to clear these we must put the tip in the water and keep pressing the pipette so all the solution clears out.
3. Put small beaker into vortexer and turn on for 5 - 10 seconds until the solution is mixed.
4. Before each extraction of nanoparticles, vortex the nanoparticle solution to ensure it is homogeneous.
5. Repeat for all concentrations.

#### Equipment List (So Far)

- Pipette: European Instruments Pipetman CL50215 20-200  $\mu$ l
- Pipette: European Instruments Pipetman H3X018102 0.5-100 $\mu$ l
- Small Beakers: 1.5ml Safe Lock Tubes Eppendorf
- Vortexer: SLS Lab Basics 220-240V 44W Output 50-60Hz 0.4A
- Nitrocellulose Membranes: Blue (unknown), Yellow (Bio-Rad 0.45 $\mu$ m #1620114)

#### Possible Errors

- Some solution left in pipette
- Human error on measurement as pipette done in stages
- Parallax error on pipette
- Bubbles in pipette
- Extra drops on outside of pipette

NOTE: All beakers and membranes MUST BE LABELLED with correct letter reference. Also check that there is roughly the same amount of solution in each as they should all be the same.

#### Constructing Membranes Method

1. Cut membranes into 16 2x3cm sheets.
2. Place 5 $\mu$ l of one of A-P onto each membrane.
3. Leave to dry overnight

NOTE: We have deposited some extra particles that we know will absorb our particular laser. These are:

- 780nm Nanorods
- 615nm Nanorods
- 780nm Nanostar

**25/02/2019 - Ivan Popov and Jennifer Lin - IN LAB UCL**

Todays Aims:

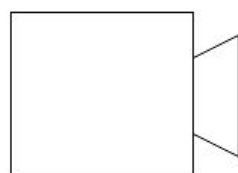
- Set up the experiment (IR Camera)
- Test the set up

Equipment:

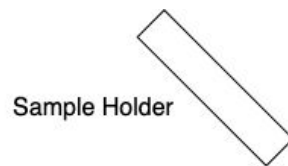
- Testo 875i - Thermal imager
- Class 3B 780nm, 80mW CW
- Laser diode controller, Tech Spin
- Sample holders
- Mirrors
- Semi-transparent mirror for power attenuation
- THOR LABS PM100D Optical Power and Energy Meter

Actual power output of laser is 31mW. Temperature has reached roughly 45°C after approximately 2 minutes of being exposed to the laser (Sample C, blue membrane).

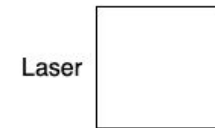
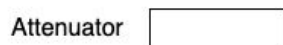
Blue membrane without nanoparticles has been exposed to the laser for 6 minutes but the temperature has only gone up to 24.3°C from 23.7 °C



Thermal Camera



Sample Holder



## EXPERIMENTAL SET UP DIAGRAM

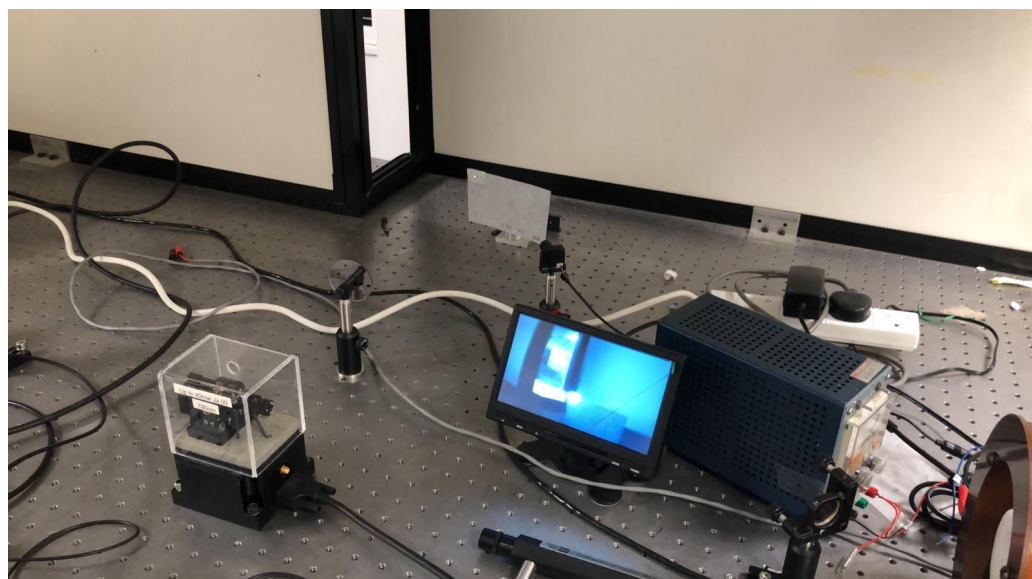
**27th February 2019 - Sean MacBride and Grace Hymas - IN LAB UCL**

Aims:

- Expose membranes to the laser with thermochromic sheets attached.
- Observe the colour change and use a higher range thermochromic sheet if necessary.

Method:

- Attach membrane to lowest temperature range thermochromic sheet using tape (non-permanent).
- Attach to stand and align with laser.
- Turn the laser on for 5 minutes.
- Observe colour change in thermochromic sheet, if there is a clear colour change, change to a higher range thermochromic sheet and repeat the experiment.
- Repeat until no colour change is observed, from this the temperature of the nanoparticles can be assumed.
- NOTE: a control must be performed first with a membrane with no nanoparticles deposited.



## EXPERIMENTAL SET UP

**Results:**

NOTE: Intensity of laser measured to be 31mW after 5 minutes of control test time.

Experimental Run Number	Membrane (Blue or Yellow)	Nanoparticle Type (A-P)	Thermochromic Sheet Range (°C)	Time (Minutes)	Observations
-------------------------	---------------------------	-------------------------	--------------------------------	----------------	--------------

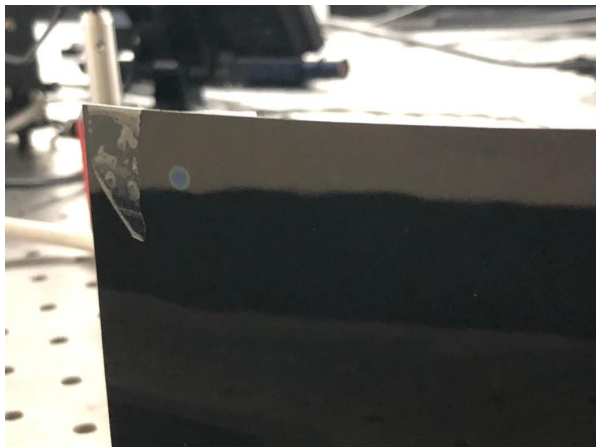
1	B	None (Control)	30 - 35	5	No change in colour
2	B	H	30 - 35	5	No change in colour
3	B	H	30 - 35	15	Change in colour after 8min45sec. Final colour change very faint green.
4	B	None (Control)	30-35	15	Colour change seen similar to Run 4.
5	B	Nanorods 780	35-40	15	Widest colour change so far. Donut shape.

NOTE: Ask which wavelengths these particles are meant to interact with. How sharp is the peak of the laser and particle wavelengths? They will not just be a specific wavelength, but a band.

Diode Laser 440mW theoretical output 780nm peak emission



CONTROL SHEET



WITH NANORODS



WITHOUT NANORODS

**4th March 2019 - Sean MacBride and Grace Hymas - IN LAB UCL**

Aims:

- Expose plain membrane to the laser and take the measurements of the temperature using thermal camera
- Expose membranes with nanoparticle solution to the laser and take the measurements of the temperature using thermal camera

Equipment:

- Testo 875i Thermal Imager

Method:

- Attach a plain membrane to the stand and align with the laser
- Place the thermal camera to face the membrane stand
- Turn on laser for 15 minutes

- Measure the temperature of the membrane with the thermal camera
- Take down the readings of temperature every 60 seconds

Results:

NOTE: Intensity of laser measured to be 32 mW after 15 minutes of control test time.

These were taken over 15 minutes with a thermal image picture taken every minute.

#### **Experimental Run 1**

**Membrane:** Blue

**Nanoparticles:** None

#### **Experimental Run 2**

**Membrane:** Blue A

**Nanoparticles:** Iron Oxide Fe<sub>3</sub>O<sub>4</sub>, Small 10mg/ml

**Started taking picture at:** 15:01

**Last image:** 0097

#### **Experimental Run 3**

**Membrane:** Blue B

**Nanoparticles:** Iron Oxide Fe<sub>3</sub>O<sub>4</sub>, Small 10mg/ml

**Started taking picture at:** 15:18

**Last image:** 00112

NOTE: between images 0098 and 0099 the temperature scale was changed from 20-40 to 20-60

#### **Experimental Run 4**

**Membrane:** Blue C

**Nanoparticles:** Iron Oxide Fe<sub>3</sub>O<sub>4</sub>, Small 10mg/ml

**Started taking picture at:** 15:35

**Last image:** 00126

#### **Experimental Run 5**

**Membrane:** Blue D

**Nanoparticles:** Iron Oxide Fe<sub>3</sub>O<sub>4</sub>, Small 10mg/ml

**Last image:** 00141

#### **Experimental Run 6**

**Membrane:** Blue E

**Nanoparticles:** Iron Oxide Fe<sub>3</sub>O<sub>4</sub>, Large 15mg/ml

**Last image:** 00156

NOTE: Intensity of laser measured to be 32 mW

#### **Experimental Run 7**

**Membrane:** Blue F

**Nanoparticles:** Iron Oxide Fe<sub>3</sub>O<sub>4</sub>, Large 15mg/ml

**Last image:** 00171

### Experimental Run 8

**Membrane:** Blue G

**Nanoparticles:** Iron Oxide Fe<sub>3</sub>O<sub>4</sub>, Large 15mg/ml

**Last image:** 00188

### Experimental Run 9

**Membrane:** Blue H

**Nanoparticles:** Iron Oxide Fe<sub>3</sub>O<sub>4</sub>, Large 15mg/ml

**Last image:** 00203

### 07/03/2019 - Ivan Popov - IN LAB RI

Todays Aims:

- Produce solutions with various concentrations from the available nanoparticles.
- Deposit solutions onto membranes.

### Calculations

Our solution of Fe<sub>3</sub>O<sub>4</sub> small contains 10µg/ml Fe<sub>3</sub>O<sub>4</sub>. Therefore to dilute our required concentration of 20µg/ml we must calculate:

$$\frac{20}{10000} \times 3000 = 6\mu l$$

So if we take 6µl of solution we will get 60µg of the nanoparticles. General formula:

$$\frac{\text{required concentration}}{\text{given concentration}} \times 3000$$

Then we can add the remaining solution (water) to make the total amount 3000µl. In the case of our example, we would use 2994µl of water.

Required Concentration (µg/ml)	Required Amount of Nanoparticle in µg			
	Iron Oxide Fe <sub>3</sub> O <sub>4</sub>		Zinc Ferrite Zn0.4Fe2.6O4	
	Small 10mg/ml	Large 15mg/ml	Small 7.3mg/ml	Large 7.5mg/ml
5	α1 1.50	β1 1.00	γ1 2.05	δ1 2.00
10	α2 3.00	β2 2.00	γ2 4.11	δ2 4.00
15	α3 4.50	β3 3.00	γ3 6.16	δ3 6.00

α1: 1.50µg with 2998.50µg water

α2: 3.00µg with 2997.00µg water

α3: 4.50µg with 2995.50µg water

β1: 1.00µg with 2999.00µg water

β2: 2.00µg with 2998.00µg water

β3: 3.00µg with 2997.00µg water

$\gamma_1$ : 2.05 $\mu\text{g}$  with 2997.95 $\mu\text{g}$  water  
 $\gamma_2$ : 4.10 $\mu\text{g}$  with 2995.90 $\mu\text{g}$  water  
 $\gamma_3$ : 6.15 $\mu\text{g}$  with 2993.85 $\mu\text{g}$  water  
 $\delta_1$ : 2.00 $\mu\text{g}$  with 2998.00 $\mu\text{g}$  water  
 $\delta_2$ : 4.00 $\mu\text{g}$  with 2996.00 $\mu\text{g}$  water  
 $\delta_3$ : 6.00 $\mu\text{g}$  with 2994.00 $\mu\text{g}$  water

NOTE: Membranes were dried in the oven at 55°C for approximately 30 minutes.

**07/03/2019 - Grace Hymas and Sean MacBride - IN LAB UCL**

Changes this session:

- 3 minute run time now with 30 second interval between thermal camera images
- Experimental set up changed such that the thermal camera can be mounted behind the laser instead of hand held. This means distance is constant and focus should be better as focus was affecting the results in previous runs.
- Thermal camera must be at an angle to the laser so that the camera does not become damaged.

PLEASE NOTE: All raw data can be found in the 'Membrane Study' files on the shared drive.

NOTE: Random fluctuations in laser power when tested approx plus minus 2mW



Experimental run 10 repeated as the filter was removed as it was not thought it was doing anything as low power laser, however laser power was fluctuating (from around 35mW to 31 mW).

Experimental run 17 repeated as 2 images in the run not saved properly.

Experimental run 23 restarted as not centred, also this paper slightly bent.

IGNORE 417 THIS WAS TAKEN AT THE WRONG TIME

Experimental Run	Membrane		Image Number		Laser Power / mW
	Type	Colour	First	Last	
10	A	Yellow	204	209	36
10B	A	Yellow	210	215	31
11	B	Yellow	216	221	31
12	C	Yellow	222	227	31
13	D	Yellow	228	233	30
14	E	Yellow	234	239	31
15	F	Yellow	240	245	30
16	G	Yellow	246	251	30
17	H	Yellow	252	255	30
17B	H	Yellow	262	267	30
18	I	Yellow	256	261	30
19	J	Yellow	268	273	30
20	K	Yellow	274	279	30
21	L	Yellow	280	285	30
22	M	Yellow	286	291	30
23	N	Yellow	293	298	31
24	O	Yellow	299	304	30
25	P	Yellow	305	310	31
26	I	Blue	311	316	31
27	J	Blue	317	322	31
28	K	Blue	323	328	30.5
29	L	Blue	329	334	30
30	M	Blue	335	340	31
31	N	Blue	341	346	31

32	O	Blue	347	351	30
33	P	Blue	352	357	30
34	CONTROL	Blue	358	363	31
35	CONTROL	Yellow	364	369	31
36	615NR	Blue	370	375	30
37	780NR	Blue	376	381	31
38	780NS	Blue	382	387	30
39	$\alpha$ 1	Yellow	388	393	30
40	$\alpha$ 2	Yellow	394	399	31
41	$\alpha$ 3	Yellow	400	405	31
42	$\beta$ 1	Yellow	406	411	30
43	$\beta$ 2	Yellow	412	418	30
44	$\beta$ 3	Yellow	419	424	31
45	$\gamma$ 1	Yellow	425	430	30
46	$\gamma$ 2	Yellow	431	436	30
47	$\gamma$ 3	Yellow	437	442	32
48	$\delta$ 1	Yellow	443	448	30
49	$\delta$ 2	Yellow	449	453	31
50	$\delta$ 3	Yellow	454	459	30
51	$\alpha$ 1	Blue	460	465	31
52	$\alpha$ 2	Blue	466	471	30
53	$\alpha$ 3	Blue	472	477	31
54	$\beta$ 1	Blue	478	483	32
55	$\beta$ 2	Blue	484	489	32
56	$\beta$ 3	Blue	490	495	31
57	$\gamma$ 1	Blue	496	500	30
58	$\gamma$ 2	Blue	501	506	31
59	$\gamma$ 3	Blue	507	512	31
60	$\delta$ 1	Blue	513	518	32
61	$\delta$ 2	Blue	519	524	30

62	δ3	Blue	525	530	31
----	----	------	-----	-----	----

## 8.5 Minutes

### 8.5.1 15/1 Meeting

Meeting Date: 15/01/2019.

The Chair: Jennifer Lin.

Minute Taker(s): Sean MacBride.

Members Present: Prof Thanh Nguyen, Grace Hymas, Sean MacBride, Jennifer Lin, Anja Rellstab, Abigail Goh, Amritpal Basi, Wenhao Wu, Ivan Popov.

Agenda:

General availability to visit laboratory

Data analysis techniques

Laser discussion

Group Structure

Start Time: 15:08.

Meeting Log:

15:08-15:10. Introductions.

15:10-15:12. Introduce main questions.

15:12-15:15. Sean: General availability to visit lab.

Several will go to the lab on Wednesday, time TBD.

Ivan, Grace, Sean

15:15-15:19. Anja: Beginning this project.

Work backwards from building the poster. We get as much time as we need in the lab.

Whole group

15:19-15:21. Grace: Determining availability to visit lab.

Wednesday and Friday at 2 (wait on email confirmation).

Grace

15:21-15:27. Ivan: Data analysis techniques.

Light density monitor, phone techniques, look through literature, potentially develop our own program.

Ivan

15:27-15:29. Abby: Laser discussion.

Laser requires a safety course, risk assessment to approve the laser for use in labs.

Abby

15:29-15:31. Thanh: Lab discussion.

Located at Green Park Station Royal institution lab.

15:31-15:34. Future Availability.

Availability changes week to week, we will shoot to meet after the lab visit.

Ivan, Grace

15:34-15:36. Thanh: Call to lab.

Unavailable to talk due to service.

15:36-15:40. Group Structure.

Dynamic structure, we should get a rough plan set up soon.

End time: 15:40.

### 8.5.2 25/1 Meeting

Meeting Date: 25/01/2019.

The Chair: Sean MacBride.

Minute Taker(s): Amritpal Basi.

Members Present: Prof Thanh Nguyen, Grace Hymas, Sean MacBride, Jennifer Lin, Anja Rellstab, Abigail Goh, Amritpal Basi, Wenhao Wu, Ivan Popov.

Agenda:

Future of Project/Project Changes

Lab Safety Paperwork

Next Steps

Start Time: 16:11.

Meeting Log:

16:11-16:13. All: Introductions.

Membrane discussion.

16:13-16:48. Thanh: Future of Project/Project Changes.

300 mw/cm<sup>2</sup> laser is what we should look for (although intensity still may be considered high), investigate postgraduate lab/Research Lab, Lab on 3rd floor as potential laser substitutes. Need to see if available and get wavelengths, frequency, energy per area of the laser. How to quantify the signal, both from a hardware (most likely a phone as that has a built in camera to take a picture of the strip) and a software (data processing of the color intensity to notify the user of the action required such as few days rest or go to the hospital). Additionally get it down to just a simple strip image to image intensity.

Abby, Ivan, Grace

16:48-16:49. Grace: Lab Safety Paperwork.

Get it signed, we need another one for whatever lab we will use.

Grace

16:49-16:51. Ivan: Next Steps.

Lab visit next week, get a laser available.

Ivan, Grace, Sean

16:51-16:59. All: Debrief.

Literature review should be started, programmes that can decipher colour intensity to be investigated. Lab visit to begin assembling LFAs also nitrocellulose membranes alternatives could be looked into.

End time: 16:52.

PI's feedback: The group should spread to other areas, as 2 group on membranes is not the best used of human resources. Great idea to look for laser source in physics, showing initiative, and effectively how one should work in collaborative spirit. The

team should also look for how to quantify the density of the signal.

### 8.5.3 1/2 Meeting

Meeting Date: 01/02/2019.

The Chair: Grace Hymas.

Minute Taker(s): Sean MacBride.

Members Present: Grace Hymas, Sean MacBride, Jennifer Lin, Anja Rellstab, Abigail Goh, Amritpal Basi, Wenhao Wu, Ivan Popov.

Agenda:

Lab update

Inquires

Side project research

Laser

Start Time: 16:03.

Meeting Log:

16:03-16:09. All: Introductions.

Setting deadlines for pieces of work and uploading more content onto the google drive including any write ups. Peer review allocations done, Jennifer and Anja to schedule a time in order to collaborate with another group. Literature review deadline set for Tuesday 5th of Feb.

Amritpal, Jenifer, Abby, Anja and Wu

16:09-16:20. Ivan/Grace/Sean: Lab update.

Some materials have been collected. Image and software giving intensity of colour of strip has been researched with a write up (side project). Currently in the lab there is only blue membranes which we can't use so white membranes are scheduled to be ordered. Once this is done assembly of the LFAs can begin.

16:20-16:22. All: Inquires.

Need to find details about finding a suitable laser and lab. Follow up on the order of membranes and an infrared camera (maybe in high energy physics department).

Abby, Wu

16:22-16:27. All: Side project research.

Looking into side projects such as designing a UI for the mobile phone application that reads LFS test line. This can include the calibration curve and a qualitative and quantitative output such as "take a few days rest".

Amritpal

16:27-16:28. All: Laser.

Follow up on the risk assessment for laser.

16:28-16:35. All: Debrief.

Tasks for everyone now assigned with a small research side task.

End time: 16:35.

#### 8.5.4 6/2 Meeting

Meeting Date: 06/02/2019.

The Chair: Grace Hymas.

Minute Taker(s): Sean MacBride.

Members Present: Grace Hymas, Sean MacBride, Jennifer Lin, Anja Rellstab, Abigail Goh, Amritpal Basi, Wenhao Wu, Ivan Popov.

Agenda:

Laser discussion

Planning for Friday meeting

Start Time: 14:02.

Meeting Log:

14:02-14:18. All: Introductions.

Need to find a rigid structure for everyone's work load, now the literature review is done there are some aspects that can be included such as a laser section, a new possible side project idea 'how nanoparticles can be used to treat diseases and how the magnetic field can be detected. Finally the lab book will be written up.

14:18-14:25. All: Laser discussion.

Finding out which lab is available with a suitable laser that will be used on the LFAs.

14:25-14:35. All: Planning for Friday meeting.

Going over the agenda for Friday meeting with the PI.

End time: 14:35.

#### 8.5.5 8/2 Meeting

Meeting Date: 08/02/2019.

The Chair: Sean MacBride.

Minute Taker(s): Amritpal Basi.

Members Present: Prof Thanh Nguyen, Grace Hymas, Sean MacBride, Jennifer Lin, Abigail Goh, Amritpal Basi, Wenhao Wu, Ivan Popov.

Agenda:

Lit Review Results and addendums

Laser Availability Update

Experimental methods progress

Peer Review Status

Membrane purchase Update

App Design update

Moving forward

Start Time: 16:34.

Meeting Log:

16:34-16:40. Wu: Lit Review Results and Addendums.

Membrane selection, sensitivity and laser research (found one at 110mW for £30) however if it meets european standards needs to be checked.

16:40-16:44. Abby: Laser Availability Update.

3b laser in the physics department however ungrads aren't allowed to use it, Nick following with a meeting on monday up with central safety policy to see if that can be overturned. However Thitiwat may be able to use the laser (needs to be followed up).

16:44-16:48. Grace: Experimental Methods Progress.

Got an online lab book that can be accessed, files contained in a google drive. Order of membranes will be processed within 2-3 days ordering to the office (Ask Neil Skipper).

16:48-16:49. Anja & Jennifer: Peer Review Status.

5-8 questions emailed to the group to provide a reflection of the group, Anja is going back for a second meeting.

16:49-16:52. Amritpal: App Design update.

Technical imaging processing software ImageJ and which can measure intensity, standard deviation etc. Using a color marker as test line can be under different lighting and environments so this will help provide an accurate output. Calibration curve need to be insured.

Amritpal, Ivan

16:52-16:54. Ivan: Thermochromic Sheets Placement.

Looked into thermochromic placement so antibodies can be absorbed, best placement is under LFAs and not a zebra placement.

16:54-16:56. All: Moving forward.

Sort out laser problems, Get IR camera, get membranes and everything ordered. Humidity control needed to be looked into for membrane preparation.

End time: 16:57.

PI's feedback: You have made good progress, and the workload has been shared among the members. You have shown your own initiative in dealing with issues such as health and safety when using laser. You have also started to write up the methodology, and share with group members, that would help in final write up. You may need to have one person or two persons who is/are capable of summarising all different parts of the projects to write up a coherent report and prepare for a poster. It would be nice that you can have a sample that can be scanned and recognised by the app for audience to try on the presentation day.

### 8.5.6 8/3 Meeting

Meeting Date: 08/03/2019.

The Chair: Ivan Popov.

Minute Taker(s): Amritpal Basi.

Members Present: Prof Thanh Nguyen, Grace Hymas, Sean MacBride, Jennifer Lin, Abigail Goh, Amritpal Basi, Wenhao Wu, Ivan Popov.

Agenda:

Introduction Update

App Design Update

Lab Update

Weekend Data Analysis Plan

Distributions of Sections for Write Up

Start Time: 17:15.

Meeting Log:

17:15-17:19. Anja & Jennifer: Introduction and Group Report Update.

Introduction is finished, looking at the structure now for the report. Going into detail in uses, laser theory, nanoparticles and applications. Figures acquired but no tables (have been condensed into writing). Including general applications in introductions and not discussion allowing for a solid background information.

17:19-17:30. Ivan, Sean & Grace: Lab Update.

Nanorods and nanostars tested to test. Some data acquired without thermal camera (pictures shown) data analysis have yet to be finished and all raw data acquired. Using control membrane there was an increase in 12-13 degrees celcius with final temp of 40-50. 400 readings acquired with thermal camera.

17:30-17:35. Thanh: Roadmap.

Providing detail for app using image J and providing a detailed roadmap.

17:35-17:44. Amritpal: App Design update.

Technical imaging processing software ImageJ and which can measure intensity, standard deviation etc. Using a color marker as test line can be under different lighting and environments so this will help provide an accurate output. Calibration curve need to be insured.

17:44-17:45. Ivan: Weekend Data Analysis Plan.

Determining limit of detection and distribution of work. Data analysis and method to be completed soon. Laser setup done on sketchup.

End time: 17:50.

PI's feedback: You have made good progress, and the workload has been shared among the members. You have shown your own initiative in dealing with issues such as health and safety when using laser. You may need to have one person or two persons who is/are capable of summarising all different parts of the projects to write up a coherent report and prepare for a poster. It would be nice that you can have a sample that can be scanned and recognised by the app for audience to try on the presentation day.

### 8.5.7 14/3 Meeting

Meeting Date: 14/03/2019.

The Chair: Ivan Popov.

Minute Taker(s): Amritpal Basi.

Members Present: Prof Thanh Nguyen, Grace Hymas, Sean MacBride, Jennifer Lin, Abigail Goh, Amritpal Basi, Wenhao Wu, Ivan Popov.

Agenda:

Data Analysis Update

Planning on Handing in the Hard Copy of the Report

Current Data Analysis and App Design Review

Final Questions

Start Time: 11:05.

Meeting Log:

11:05-11:07. Ivan: Introductions.

Almost finished writing the formal report, just need to write up everything in Latex.

11:07-11:15. Grace: Data Analysis Update.

Data analysis almost done, kai squared fits calculated too, remains to be written up in Latex. Emailed our data analysis to PI. Had to rewrite some parts with respect to new data analysis, some space left to fill in conclusion.

11:15-11:17. All: Planning on Handing in the Hard Copy of the Report.  
scheduling a time to drop off the report.

11:17-11:49. All: Current Data Analysis and App Design Review.

PI going over our data analysis discussing our findings. Linear Fit did not work as it produces negative limits of detection so a logarithmic plot was instead used. On the figure explain the condition of experiment (for example 3 minute exposure and how often images where taken). Explain Hex colour code.

11:49-11:55. All: Final Questions.

Give remaining resources remaining Thithawat so there is no wastage. Hand in report tomorrow. Information on poster design.

Amritpal, Ivan

End time: 11:55.

PI's feedback: The students are getting on well with preparing of the report. Advice was given to how to prepare report with TOC, figure legend, and how to prepare poster. I am happy with the progress so far.